Pontifícia Universidade Católica do Rio Grande do Sul

Programa de Pós-Graduação em Biologia Celular e Molecular

Leonardo Krás Borges Martinelli

GMP redutase de *Escherichia coli*: mecanismos cinéticos, catalíticos e químicos e a termodinâmica da formação do complexo binário de ligação enzima-ligante

Porto Alegre

2011

Leonardo Krás Borges Martinelli

GMP redutase de *Escherichia coli*: mecanismos cinéticos, catalíticos e químicos e a termodinâmica da formação do complexo binário de ligação enzima-ligante

Tese apresentada como requisito para obtenção de grau de Doutor pelo Programa de Pós-Graduação em Biologia Celular e Molecular da Faculdade de Biociências da Pontifícia Universidade Católica do Rio Grande do Sul

Orientador: Prof. Dr. Diógenes Santiago Santos

Co-orientador: Prof. Dr. Luiz Augusto Basso

Porto Alegre

2011

Leonardo Kras Borges Martinelli

GMP redutase de *Escherichia coli*: mecanismos cinéticos, catalíticos e químicos e a termodinâmica da formação do complexo binário de ligação enzima-ligante

Tese apresentada como requisito para obtenção de grau de Doutor pelo Programa de Pós-Graduação em Biologia Celular e Molecular da Faculdade de Biociências da Pontifícia Universidade Católica do Rio Grande do Sul

Aprovada em _____de_____de_____.

BANCA EXAMINADORA

Dr Alejandro Miguel Katzin - USP

_____

Dr Giancarlo Pasquali – UFRGS

_____

Dra Maria Martha Campos – PUCRS (relatora)

_____

Agradecimentos

Ao Prof. Diogénes Santiago Santos, agradeço pela oportunidade de integrar seu grupo de pesquisa, pela orientação do trabalho e, por contribuir e proporcionar um maior aprendizado e uma melhor formação acadêmica.

Ao Prof. Luiz Augusto Basso, agradeço pelo conhecimento compartilhado, pelos ensinamentos passados e pelas correções e sugestões para que o trabalho fosse finalizado.

Aos Drs Eraldo Batista Jr, Claudia Paiva Nunes e Gaby Renard por todo o conhecimento, conselhos e ajudas indispensáveis para o trabalho, mas principalmente pela amizade ao longo do tempo.

Gostaria de agradecer especialmente aos amigos Christiano, Leonardo, e Rodrigo pela amizade ao longo dos anos, pelos momentos de diversão e descontração que foram fundamentais para superar os momentos difíceis. A todos os colegas do Centro de Pesquisa em Biologia Molecular e Funcional e da Quatro G, que diretamente ou indiretamente colaboraram com o trabalho, além da amizade e companheirismo de todos.

Gostaria de agradecer aos meus pais, que ao longo dos anos sempre me incentivaram e me deram todo o apoio e suporte necessário para a realização dessa etapa, e por todo carinho e compreensão ao longo do tempo.

Gostaria de agradecer em especial a uma pessoa, a minha namorada Clarissa Medeiros, que foi fundamental para essa conquista, pelo amor, carinho, compreensão, e paciência, ao longo do tempo.

A new type of thinking is essential if mankind is to survive and move toward higher levels.

Albert Einstein

Resumo

A enzima guanosina monofosfato (GMP) redutase catalisa a deaminação redutiva do GMP à inosina monofosfato (IMP). GMP redutase possui um papel importante na conversão dos nucleosídeos e nucleotídeos derivados de guanina a nucleotídeos de adenina. Além desse fato, como parte da via de salvamento de purinas, também participa da reutilização de bases livres intracelulares. Nesse trabalho, mostramos a clonagem, a expressão e a purificação da GMP redutase codificada pelo gene *gua*C de *Escherichia coli* a fim de determinar seu mecanismo cinético; bem como as características químicas e termodinâmicas da reação catalisada. Estudos de velocidade inicial e titulação de calorimetria isotérmica demonstraram que a GMP redutase possui um mecanismo cinético bi-bi ordenado, no qual o GMP liga primeiro à enzima, seguido pela ligação do NADPH; o $NADP^+$ se dissocia primeiro, seguido pela liberação do IMP. A titulação calorimétrica também mostrou que a ligação do GMP e IMP são processos termodinamicamente favoráveis. Perfis de pH demonstraram grupos com valores de *pK* aparentes de 6,6 e 9,6 envolvidos na catálise, valores de *pK* de 7,1 e 8,6 importantes para ligação do GMP e um valor de *pK* de 6,4 importante para ligação do NADPH. Efeito isotópico primário demonstrou que a transferência do hidreto contribui para a etapa limitante da reação, enquanto que os efeitos isotópicos do solvente provêm de um único local de protonação que possui um papel modesto na catálise. Efeito isotópico múltiplo sugere que as etapas de protonação e transferência do hidreto ocorrem no mesmo estado de transição, fornecendo evidência de um mecanismo *concerted*. Os dados de cinética em estado pré-estacionário indicam que a liberação do produto não contribui para a etapa limitante da reação catalisada pela GMP redutase de *E. coli*. Em conjunto, os resultados mostram que a reação catalisada pela GMP redutase segue um mecanismo sequencial e ordenado, onde a transferência do hidreto e do próton ocorrem no mesmo estado de transição. Os resultados aqui apresentados foram os primeiros a evidenciar o mecanismo cinético da GMP redutase, bem como, os resíduos fundamentais para catálise e/ou ligação, além de fornecer informações sobre o estado de transição da reação.

Abstract

Guanosine monophosphate (GMP) reductase catalyzes the reductive deamination of GMP to inosine monophosphate (IMP). GMP reductase plays an important role in the conversion of nucleoside and nucleotide derivatives of guanine to adenine nucleotides. In addition, as a member of the purine salvage pathway, it also participates in the reutilization of free intracellular bases. Here we present cloning, expression and purification of *Escherichia coli guaC*-encoded GMP reductase to determine its kinetic mechanism, as well as chemical and thermodynamic features of this reaction. Initial velocity studies and isothermal titration calorimetry demonstrated that GMP reductase follows an ordered bi-bi kinetic mechanism, in which GMP binds first to the enzyme followed by NADPH binding, and $NADP^+$ dissociates first followed by IMP release. The isothermal titration calorimetry also showed that GMP and IMP binding are thermodynamically favorable processes. The pH-rate profiles showed groups with apparent p*K* values of 6.6 and 9.6 involved in catalysis, and p*K* values of 7.1 and 8.6 important to GMP binding, and a p*K* value of 6.4 important for NADPH binding. Primary deuterium kinetic isotope effects demonstrated that hydride transfer contributes to the rate-limiting step, whereas solvent kinetic isotope effects arise from a single protonic site that plays a modest role in catalysis. Multiple isotope effects suggest that protonation and hydride transfer steps take place in the same transition state, lending support to a concerted mechanism. Pre-steady-state kinetic data suggest that product release does not contribute to the rate-limiting step of the reaction catalyzed by *E. coli* GMP reductase.

Lista de Siglas

RNA – ácido ribonucleico

DNA – ácido desoxirribonucleico

ATP – trifosfato de adenosina

GTP – trifosfato de guanosina

FAD – flavina adenina dinucleotídeo

NAD – nicotinamida adenina dinucleotídeo

cAMP – monofosfato de adenosina cíclico

cGMP – monofosfato de guanosina cíclico

PRPP – 5-fosforribosil-α-1-pirofosfato

10-formil-THF – 10-formiltetrahidrofolato

IMP – monofosfato de inosina

XMP – monofosfato de xantina

E. coli – *Escherichia coli*

APRT – adenina fosforribosiltransferase

PPi – pirofosfato

GPRT – guanina fosforribosiltransferase

HPRT – hipoxantina fosforribosiltransferase

PNP – purina nucleosídeo fosforilase

NADPH – nicotinamida adenina dinucleotídeo fosfatado

KDa – Quilodáltons

ESI-MS – do inglês *electrospray ionization mass spectrometry*

IPTG – isopropil β-D-tiogalactopiranosídeo

SDS-PAGE – do inglês *sodium dodecyl sulfate polyacrylamide gel electrophoresis*

SUMÁRIO

CAPÍTULO 1

Introdução

1.1 Nucleotídeos

1.2 Metabolismo de purinas e pirimidinas

1.2.1 Via *de novo* de purinas

1.2.2 Via de salvamento de purinas

1.2.3. Interconversão de purinas

1.3 GMP redutase

INTRODUÇÃO

1.1 Nucleotídeos

Nucleotídeos são moléculas que possuem uma diversidade estrutural extensa, existindo oito variedades comuns de nucleotídeos, cada uma composta por uma base nitrogenada ligada a uma pentose (açúcar de cinco carbonos), a qual possui pelo menos um grupo fosfato. A pentose pode ser tanto uma ribose, presente no ácido ribonucleico (RNA), quanto uma desoxirribose, componente do ácido desoxirribonucleico (DNA) (Alberts, 2010). As bases nitrogenadas são moléculas planares, aromáticas e heterocíclicas derivadas de purinas ou de pirimidinas. As purinas mais comuns são a adenina (A) e guanina (G), e as principais pirimidinas são a citosina (C), a uracila (U) e a timina (T). As purinas são ligadas à pentose pelo átomo N9, ao contrário das pirimidinas que se ligam à pentose pelo átomo N1 (Voet, 2006).

Além de componentes chaves dos ácidos nucléicos, portanto responsáveis diretos pelo armazenamento e disponibilização da informação biológica, os nucleotídeos realizam diversas outras funções bioquímicas, como o armazenamento de energia através de moléculas como o trifosfato de adenosina (ATP) e o trifosfato de guanosina (GTP). Os nucleotídeos também são componentes de alguns cofatores centrais do metabolismo como flavina adenina dinucleotídeo (FAD), nicotinamida adenina dinucleotídeo (NAD) e coenzima A, além de regular diversas rotas metabólicas através do monofosfato de

adenosina cíclico (cAMP) e do monofosfato de adenosina cíclico (cGMP), que são importantes segundos mensageiros (Voet, 2006).

1.2 Metabolismo de purinas e pirimidinas

Em *Escherichia coli*, purinas e pirimidinas podem ser sintetizadas a partir de precursores simples, através da síntese *de novo*, ou através da reciclagem de bases livres pela chamada *via de salvamento* (Smith, Marks, Lieberman, 2005). Em ambos os casos, a parte α-D-ribose-5-fosfato é derivada do 5-fosforribosil-α-1-pirofosfato (PRPP). PRPP é necessário para a biossíntese de purinas e pirimidinas, tanto pela via *de novo* quanto pela via de salvamento, além da síntese de nucleotídeos de nicotinamida e da síntese de histidina e triptofano (El Kouni, 2003).

A ingestão alimentar de bases purínicas e pirimidínicas é mínima, uma vez que a dieta contém ácidos nucleicos e o pâncreas secreta desoxirribonuclease e ribonuclease, juntamente com enzimas proteolíticas e lipolíticas. Este aspecto permite que os ácidos nucleicos digeridos sejam convertidos em nucleotídeos e o epitélio intestinal converta esses nucleotídeos em nucleosídeos, através da atividade da fosfatase alcalina. Aproximadamente 5% dos nucleotídeos ingeridos entram na circulação, tanto na forma de nucleosídeo, como na forma de base livre. Pelo fato da ingestão mínima destas importantes moléculas, a síntese *de novo* de purinas e pirimidinas é necessária (Smith, Marks, Lieberman, 2005).

1.2.1 Via *de novo* de purinas

A síntese de purinas em *E. coli* pela via *de novo* corresponde a onze etapas enzimáticas e requer seis moléculas de ATP para cada purina sintetizada (Figura 1). Os precursores que fornecem os componentes básicos para produzir nucleotídeos purínicos são a glicina, α-D-ribose-5-fosfato, glutamina, aspartato, dióxido de carbono (CO_2) e 10-formiltetrahidrofolato (10-formil-THF). A síntese *de novo* produz o monofosfato de inosina (IMP), primeiro intermediário da via, que corresponde ao nucleotídeo da base hipoxantina. Através do PRPP, o anel purínico é montado a partir de nitrogênios da amida da glutamina, do grupo amino do aspartato, de dois átomos de carbono e do grupo amino da glicina e de três moléculas de CO_2 e dos átomos de carbono de duas moléculas de 10-formil-THF (Neidhardt, 2005).

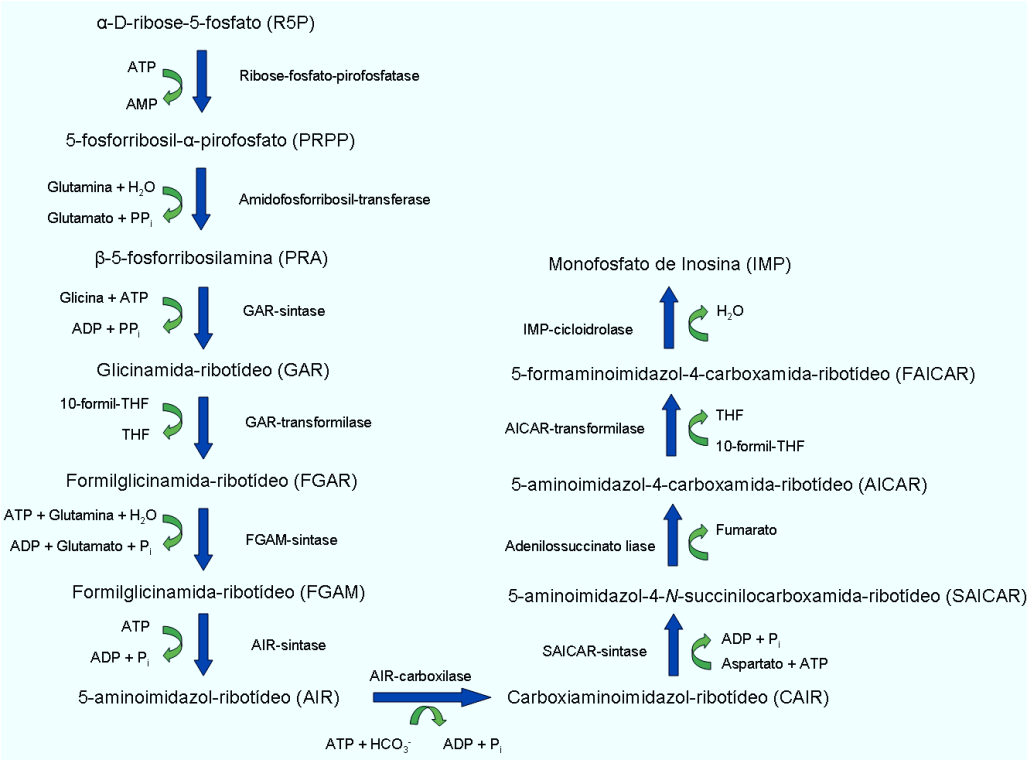

Figura 1: Síntese *de novo* de purinas em *E. coli* (Adaptado de Voet, 2006)

A molécula de IMP serve como ponto de origem para a síntese de AMP e GMP (Figura 2). O AMP é formado a partir do IMP em duas etapas enzimáticas, onde primeiro o aspartato é adicionado ao IMP para formar adenilosuccinato, numa reação catalisada pela enzima adenilosuccinato sintase (Stayton, Rudolph, Fromm, 1983). Posteriormente, fumarato é liberado do adenilosuccinato para formar AMP pela enzima adenilosuccinato liase (He, Smith, Zalkin, 1983).

O GMP também é sintetizado a partir do IMP em duas etapas enzimáticas. No primeiro passo, a base hipoxantina é oxidada pela enzima IMP desidrogenase para produzir a base xantina e o nucleotídeo monofosfato de xantina (XMP) (Gilbert, Lowe, Drable, 1979). O aminoácido glutamina doa a amina ao XMP para formar GMP, numa reação catalisada pela enzima GMP sintase (Sakamoto, Hatfield, Moyed, 1972). GMP e AMP podem ser fosforilados aos seus respectivos nucleotídeos di e trifosfatados, através de enzimas quinases especificadas (Smith, Marks, Lieberman, 2005).

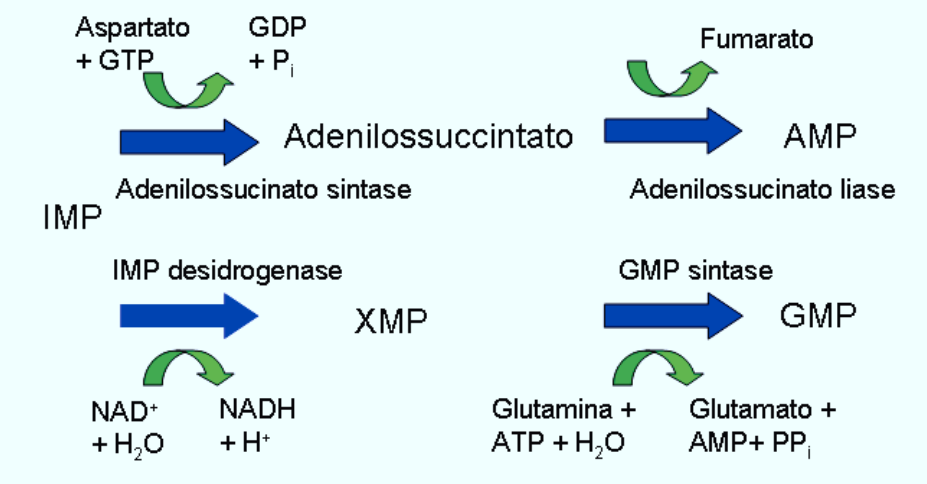

Figura 2: Síntese de AMP e GMP a partir de IMP
(Adaptado de Voet, 2006)

1.2.2 Via de salvamento de purinas

A via de salvamento realiza diversas funções, como por exemplo, a reciclagem de bases e nucleosídeos exógenos pré-formados para síntese de nucleotídeos, bem como a reutilização de bases e nucleosídeos produzidos endogenamente como resultado do metabolismo de nucleotídeos (Ducati, Breda, Basso, Santos, 2010). Uma terceira função é catabólica, uma vez que a pentose dos nucleosídeos exógenos e os grupos amino dos compostos de adenina estão disponíveis como fontes de carbono e nitrogênio respectivamente (Neidhardt, 2005).

Em *E. coli*, as bases livres e os nucleosídeos presentes no meio de cultura, quando reciclados, diminuem consideravelmente a contribuição da via *de novo* para a síntese de nucleotídeos (Houlberg, Jensen, 1983). Através da via de salvamento, bases livres como adenina, guanina e hipoxantina são convertidas em seus nucleotídeos correspondentes em um passo metabólico (Figura 3) correspondendo a uma economia de tempo e, principalmente, de energia em relação à via *de novo*, visto que as principais enzimas da rota, adenina-fosforribosiltransferase (APRT) e hipoxantina-guanina-fosforribosiltransferase (HGPRT) não utilizam ATP em suas reações (Devlin, 2007). A enzima APRT converte a base livre adenina em AMP pela transferência da parte fosforribosil do PRPP à base, com a liberação de pirofosfato (PPi) (Hershey, Taylor, 1986). Em *E. coli*, existem duas 6-oxopurinas fosforribosiltransferase correspondentes à

enzima HGPRT, a guanina–fosforribosiltransferase (GPRT) e a hipoxantina-fosforribosiltransferase (HPRT), que convertem as bases livres guanina e hipoxantina a seus respectivos nucleotídeos, pela utilização do PRPP (Hochstadt, 1978). Além da reciclagem das bases livres, a enzima purina nucleosídeo fosforilase (PNP) converte os nucleosídeos disponíveis nas suas bases correspondentes (Jensen, Nygaard, 1975), que por sua vez são convertidos aos seus respectivos nucleotídeos pelas enzimas fosforribosiltransferases (PRT). Existe uma controvérsia em relação ao papel da enzima PNP na via de salvamento, uma vez que ela converte os nucleosídeos nas suas bases e por definição essa via compreende a reutilização de tais compostos para formar nucleotídeos, papel das enzimas PRT. Portanto, o papel da PNP ainda não foi totalmente esclarecido, podendo ser classificada como uma enzima da via de salvamento ou simplesmente como parte do catabolismo de nucleosídeos.

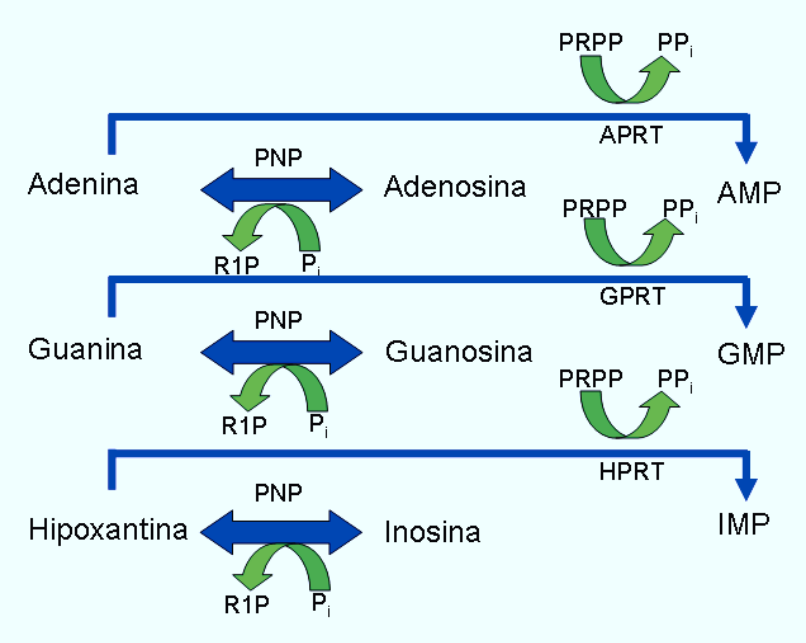

Figura 3: Via de salvamento de purinas em *E. coli*
(Adaptado de Voet, 2006)

1.2.3. Interconversão de purinas

Os nucleotídeos de adenina e guanina podem ser interconvertidos através de seu precursor comum, o IMP. A conversão ocorre através duas rotas distintas, uma vez que as reações que formam AMP e GMP a partir do IMP são irreversíveis. Compostos de adenina podem ser convertidos a nucleotídeos de guanina por duas rotas metabólicas distintas, enquanto uma enzima catalisa a conversão de GMP a IMP. Estas conversões servem para equilibrar os níveis de nucleotídeos de adenina e guanina, especialmente quando esses nucleotídeos estão presentes no meio de cultura (Neidhardt, 2005).

A conversão de AMP para IMP consiste em três passos metabólicos: primeiro a enzima 5' nucleotidase converte AMP em adenosina (Knöfel, Sträter, 1999), depois a enzima adenosina desaminase produz inosina a partir da adenosina formada (Chang, Nygaard, Chinault, Kellems, 1991) e por fim a enzima inosina quinase converte a inosina em IMP (Harlow, Nygaard, Hove-Jensen, 1995), precursor da formação do GMP. Para os compostos de guanina e xantina serem convertidos em IMP, primeiro eles devem ser metabolizados a GMP, uma vez que a desaminação do GMP é a única via que leva ao IMP (Figura 4). Essa desaminação redutiva é catalisada pela enzima caracterizada no presente trabalho, a GMP redutase, e será mais bem detalhada no próximo item.

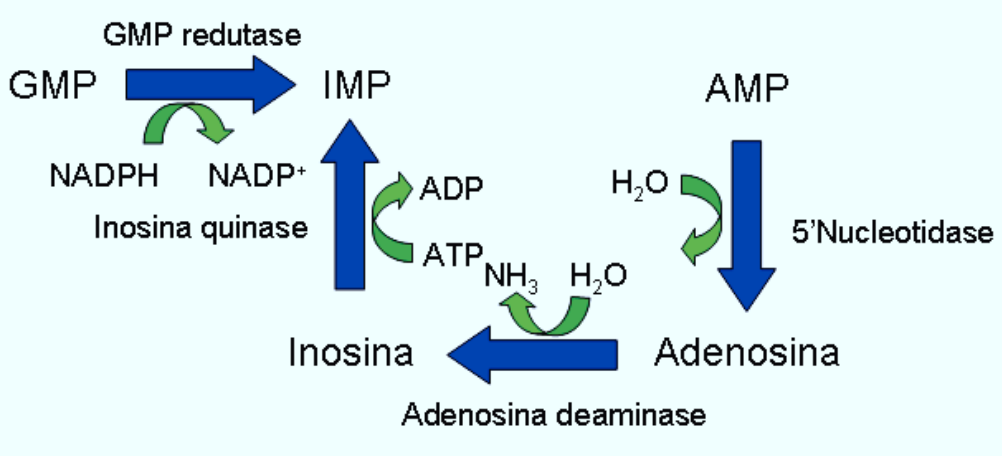

Figura 4: Interconversão de GMP e AMP através do IMP
(Adaptado de Voet, 2006)

1.3 GMP redutase

A enzima GMP redutase (NADPH:GMP oxirredutase; EC 1.6.6.8) catalisa a desaminação redutiva do GMP à IMP, com a nicotinamida adenina dinucleotídeo fosfatado (NADPH) como doador de elétron, e é codificada pelo gene *guaC,* além de possuir um papel fundamental na conversão de nucleotídeos de guanina e adenina (Andrews, Guest, 1988). Em *E. coli,* participa da via de salvamento de purinas reutilizando bases intracelulares livres, mantendo o equilíbrio entre as bases guanina e adenina (Roberts, Lienhard, Gaines, Smith, Guest, 1988). Esta enzima é fortemente inibida pelo ATP em concentrações fisiológicas, uma vez que esse nucleotídeo é o produto final da rota, porém essa inibição é completamente reversível pelo GTP (Mager, Magasanik, 1960) além de esta enzima ser inativada sob condições de escassa de bases púricas (Nygaard, 1983). Os níveis de GMP redutase são aumetados até dez vezes quando se adiciona guanina ou guanosina no meio de cultura, e esta indução é prevenida por adenina (Kessler, Gots, 1985). A enzima GMP

redutase geralmente não é necessária para o eficiente crescimento bacteriano, visto que a sua inativação não afeta a via *de novo* de purinas através de IMP (Roberts, Lienhard, Gaines, Smith, Guest, 1988). Entretanto, quando a via de IMP está bloqueada, a atividade da GMP redutase torna-se necessária para fornecer AMP quando as fontes de bases púricas são derivadas de guanina (Kessler, Gots, 1985).

A enzima GMP redutase já foi encontrada e caracterizada em diversos organismos além de *E. coli*, como por exemplo *Salmonella typhimurium* (Garber, Jochimsen, Gots, 1980), *Artemia salina* (Renart, Sillero, 1976), *Leishmania donavani* (Spector, Jones, 1982), e *Homo sapiens* (Mackenzie, Sorensen, 1973). A enzima homóloga humana representa a única etapa metabólica nas quais nucleotídeos de guanina podem ser convertidos ao precursor chave dos nucleotídeos de adenina e guanina (Spector, Jones, Miller, 1979). As enzimas GMP redutases possuem uma alta similaridade entre as espécies, sendo que se apresentam em solução na forma tetramérica, consistindo de quatro subunidades idênticas de aproximadamente 37 KDa (Figura 5).

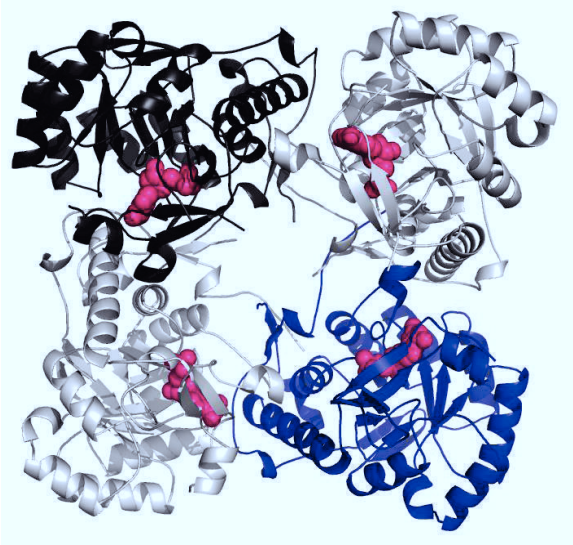

Figura 5: GMP redutase de *H. sapiens* complexada com GMP (Li et al. 2006)

A caracterização enzimática da GMP redutase torna-se necessária, uma vez que ela está envolvida na interconversão de bases púricas, sendo responsável pela conversão e o balanceamento entre os nucleotídeos de guanina e de adenina. A elucidação dos aspectos cinéticos, químicos e termodinâmicos da reação catalisada pela enzima ajudará a compreender seu o papel e sua importância no balanceamento das bases púricas.

Através da caracterização bioquímica da GMP redutase, o desenho racional de compostos (ativadores ou inibidores) possibilitará o entendimento mais amplo do papel da enzima na via de salvamento de *E. coli,* bem como a utilização de inibidores enzimáticos como alternativa para o tratamento de infecções por *E. coli* que sejam resistentes aos medicamentos de primeira escolha. Além disso, a GMP redutase de *E. coli* pode servir como modelo para o desenho de inibidores que tenham como alvo enzimas homólogas de outros organismos patogênicos, como por exemplo, *Salmonella* sp., *Shigella* sp., e *Klebsiella* sp..

A elucidação do modo de ação da GMP redutase bacteriana e a sua disponibilidade na forma recombinante pode fornecer uma ferramenta para o estudo das enzimas fosfodiesterases (PDEs). Essas enzimas catalisam a hidrólise de cAMP e cGMP (Lugnier, 2006), sendo que essa reação só é possível monitorar na presença de uma enzima acoplada, no caso GMP redutase. As PDEs são divididas em grupos de acordo com os seus substratos e as PDE5, PDE6 e PDE11 catalisam somente a hidrólise do cGMP e são alvos

molecular para tratamento de disfunção erétil, alterações visuais, regulações do comportamento e aprendizagem (Zhang, 2009).

CAPÍTULO 2

Objetivos

2.1 Objetivo Geral

2.2 Objetivos Específicos

OBJETIVOS

2.1 Objetivo Geral

Este trabalho teve como objetivo a purificação e a caracterização bioquímica e termodinâmica da enzima GMP redutase de *E. coli* a serem realizados no Centro de Pesquisas em Biologia Molecular e Funcional da PUCRS (CP-BMF) localizado no Instituto Nacional de Ciência e Tecnologia em Tuberculose (INCT-TB).

2.2 Objetivos específicos

1- Estabelecer um protocolo de purificação eficiente a fim de se obter a proteína recombinante GMP redutase para posterior determinação dos mecanismos enzimáticos;

2- Confirmar a identidade e massa da proteína através de espectrometria de massa por ESI-MS;

3- Determinar o estado oligomérico em solução da proteína recombinante GMP reductase;

4- Determinar as constantes cinéticas verdadeiras em estado estacionário da reação catalisada pela enzima GMP reductase;

5- Determinar o mecanismo cinético da reação catalisada pela enzima GMP reductase;

6- Determinar o mecanismo químico da reação catalisada pela enzima GMP reductase;

7- Determinar os parâmetros termodinâmicos de ligação aos substratos e aos produtos através de titulação isotérmica de calorimetria.

CAPÍTULO 3

Artigo

"Recombinant *Escherichia coli* GMP reductase: kinetic, catalytic and chemical mechanisms, and thermodynamics of enzyme-ligand binary complex formation"

Molecular Biosystem, 2010

Impact factor, 3,859

Molecular BioSystems

View Online
Dynamic Article Links

Cite this: DOI: 10.1039/c0mb00245c

www.rsc.org/molecularbiosystems

PAPER

Recombinant *Escherichia coli* GMP reductase: kinetic, catalytic and chemical mechanisms, and thermodynamics of enzyme–ligand binary complex formation

Leonardo Krás Borges Martinelli,[ab] Rodrigo Gay Ducati,[a] Leonardo Astolfi Rosado,[ac] Ardala Breda,[ab] Bruna Pelegrim Selbach,[ab] Diógenes Santiago Santos*[ab] and Luiz Augusto Basso*[ab]

Received 22nd October 2010, Accepted 18th January 2011
DOI: 10.1039/c0mb00245c

Published on 07 February 2011 on http://pubs.rsc.org | doi:10.1039/C0MB00245C
Downloaded by Pontificia Universidade Catolica do Rio Grande do Sul on 28 February 2011

Guanosine monophosphate (GMP) reductase catalyzes the reductive deamination of GMP to inosine monophosphate (IMP). GMP reductase plays an important role in the conversion of nucleoside and nucleotide derivatives of guanine to adenine nucleotides. In addition, as a member of the purine salvage pathway, it also participates in the reutilization of free intracellular bases. Here we present cloning, expression and purification of *Escherichia coli guaC*-encoded GMP reductase to determine its kinetic mechanism, as well as chemical and thermodynamic features of this reaction. Initial velocity studies and isothermal titration calorimetry demonstrated that GMP reductase follows an ordered bi–bi kinetic mechanism, in which GMP binds first to the enzyme followed by NADPH binding, and $NADP^+$ dissociates first followed by IMP release. The isothermal titration calorimetry also showed that GMP and IMP binding are thermodynamically favorable processes. The pH-rate profiles showed groups with apparent p*K* values of 6.6 and 9.6 involved in catalysis, and p*K* values of 7.1 and 8.6 important to GMP binding, and a p*K* value of 6.2 important for NADPH binding. Primary deuterium kinetic isotope effects demonstrated that hydride transfer contributes to the rate-limiting step, whereas solvent kinetic isotope effects arise from a single protonic site that plays a modest role in catalysis. Multiple isotope effects suggest that protonation and hydride transfer steps take place in the same transition state, lending support to a concerted mechanism. Pre-steady-state kinetic data suggest that product release does not contribute to the rate-limiting step of the reaction catalyzed by *E. coli* GMP reductase.

Introduction

Purine nucleoside and nucleotide biosynthesis is a fundamental and well-established pathway in the metabolism of avian, mammalian and microbial cells.[1] Guanosine monophosphate (GMP) reductase (NADPH:GMP oxidoreductase; EC 1.6.6.8) catalyzes the reductive deamination of GMP to inosine monophosphate (IMP)[2] (Fig. 1). GMP reductase plays an important role in the conversion of nucleoside and nucleotide derivatives of guanine (Gua) to adenine (Ade) nucleotides, and in the maintenance of the intracellular balance between Gua and Ade nucleotides.[3] As part of the purine salvage pathway, it also participates in the reutilization of free intracellular bases.[2] In *Escherichia coli*, the *guaC*-encoded GMP reductase is induced by GMP,[4] and is also regulated by cyclic adenosine monophosphate (cAMP),[5] by the intracellular ratio of purine nucleotides, and by glutamine and its analogs.[6] In addition to its role as an enzyme for the interconversion of purine nucleotides, GMP reductase provides a nitrogen source *via* its deamination activity.[6] In addition, it is inhibited by adenosine triphosphate (ATP) and is reactivated by the presence of guanosine triphosphate (GTP).[3] GMP reductase is not normally necessary for efficient bacterial growth, since the lack of its activity leaves the *de novo* synthesis of purine nucleotides *via* IMP intact.[4] However, when the route of IMP is blocked, GMP reductase activity becomes necessary to provide AMP when Gua and its derivatives are the purine sources.[7] In purine auxotroph mutants that are blocked prior to the formation of IMP, *guaC* mutations prevent the use of Gua or xanthine derivatives as sources of purine.[3]

[a] *Centro de Pesquisas em Biologia Molecular e Funcional (CPBMF), Instituto Nacional de Ciência e Tecnologia em Tuberculose (INCT-TB), Pontifícia Universidade Católica do Rio Grande do Sul (PUCRS), 6681/92-A Av. Ipiranga, 90619-900, Porto Alegre, RS, Brazil. E-mail: luiz.basso@pucrs.br, diogenes@pucrs.br; Fax: +55 51-33203629; Tel: +55 51-33203629*
[b] *Programa de Pós-Graduação em Biologia Celular e Molecular, Pontifícia Universidade Católica do Rio Grande do Sul (PUCRS), Porto Alegre, RS, Brazil*
[c] *Programa de Pós-Graduação em Medicina e Ciências da Saúde, Pontifícia Universidade Católica do Rio Grande do Sul (PUCRS), Porto Alegre, RS, Brazil*

View Online

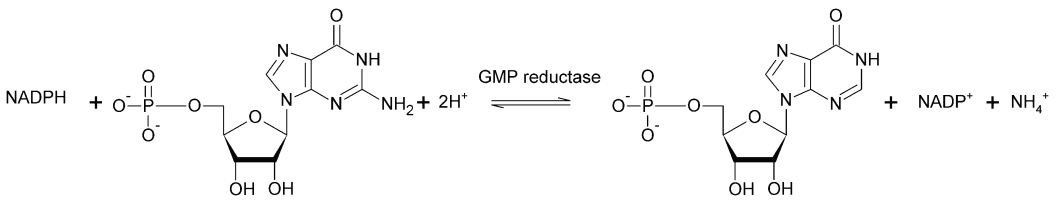

Fig. 1 Chemical reaction catalyzed by GMP reductase.

Downloaded by Pontificia Universidade Catolica do Rio Grande do Sul on 28 February 2011
Published on 07 February 2011 on http://pubs.rsc.org | doi:10.1039/C0MB00245C

GMP reductases have been found and characterized in a number of organisms, including *E. coli*,[3] *Salmonella typhimurium*,[6] *Artemia salina*,[8] *Leishmania donovani*,[9] and *Homo sapiens*.[10] The human homologue is responsible for the only known metabolic step by which Gua nucleotides can be converted to the pivotal precursor of both Ade and Gua nucleotides.[11] Human deficiency of this enzyme has not been related to any known disease, which can be explained by several possibilities, the main one being that the lack of this enzyme is invariably lethal.[12] Human GMP reductase has been identified as two isoenzymes, hGMPR1[11] and hGMPR2[2] (the second being shown to promote monocytic differentiation of HL-60 leukemia cells).[13] Salvatore and co-workers[14] studied the role of GMP reductase in non-shivering thermogenesis, a process required for the survival of rodents during cold stress, and determined that the enzyme plays a critical role in this process, evidenced by significant increases in its expression during cold exposure. GMP reductases have been shown to be involved in various biological functions, including maintenance of the balance of purine nucleotides,[3] as a possible target for antileishmanial[9] and anticancer drugs,[15] and involvement in human cell differentiation.[13] Moreover, GMP reductases are similar across the species at the amino acid level.[16] Accordingly, the need to further investigate *E. coli* GMP reductase to elucidate the kinetic, catalytic and chemical mechanisms to provide a basis on which to design species-specific inhibitors is warranted. Understanding the mode of action of *E. coli* GMP reductase may also be useful to chemical biologists interested in designing function-based chemical compounds to elucidate the biological role of this enzyme in the context of whole *E. coli* cells. In addition, availability of recombinant *E. coli* GMP reductase may provide a tool for determination of substrate specificity of cyclic nucleotide phosphodiesterases (PDEs).

Results

Amplification and cloning of the *E. coli guaC* gene

A PCR amplification product consistent with the expected size for the *E. coli guaC* (1038 bp) coding sequence was detected by agarose gel electrophoresis (data not shown), purified, and cloned into the pCR-Blunt vector. The cloned sequence was extracted from the cloning vector, purified and subcloned into the pET-23a(+) expression vector. DNA sequence identity of the fragment cloned in the expression vector was confirmed by enzyme restriction analysis and automated DNA sequencing.

Expression and purification of recombinant GMP reductase

The recombinant pET-23a(+)::*guaC* plasmid was transformed into *E. coli* BL21(DE3) host cells by electroporation.

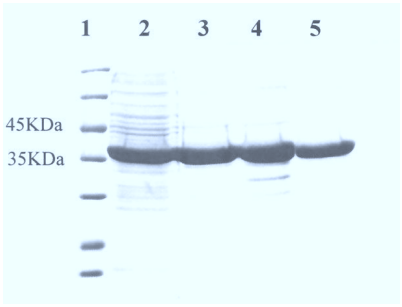

Fig. 2 SDS-PAGE (12%) analysis for the three chromatographic steps of purification of recombinant *E. coli* GMP reductase that yielded homogeneous protein. Lane 1, Molecular Weight Protein Marker (Fermentas); lane 2, crude extract; lane 3, Q-Sepharose anion exchange column; lane 4, Sephacryl S-200 size exclusion; lane 5 MonoQ High Resolution anion exchange column.

Sodium dodecyl sulfate–polyacrylamide gel electrophoresis (SDS-PAGE) analysis revealed expression of a protein in the soluble fraction with an apparent subunit molecular mass of ~38 kDa, consistent with *E. coli* GMP reductase (37 383.6 Da). The expression of the recombinant protein was monitored at different periods of cell growth after an OD_{600nm} value of approximately 0.4–0.6 was reached. The best result was achieved at 24 h of cell growth at 37 °C in LB medium without isopropyl-β-D-thio-galactopyranoside (IPTG) induction (data not shown). Recombinant GMP reductase was efficiently purified to homogeneity (Fig. 2) by a three-step purification protocol yielding 45 mg of homogeneous recombinant GMP reductase from 2.8 g of cells (Table 1). Homogeneous enzyme was stored at −80 °C with no loss of activity.

Quaternary structure analysis of *E. coli* GMP reductase

The subunit molecular mass of *E. coli* GMP reductase was determined as 37 382 Da by electrospray ionization mass spectrometry (ESI-MS) and suggests that there was no removal of the N-terminal methionine residue (theoretical molecular mass of 37 383.6 Da). Amino acid sequencing of *E. coli* GMP reductase confirmed approximately 85% of the sequence.

The protein native molecular mass was determined by gel filtration chromatography and revealed a single peak with elution volume consistent with a molecular mass of 155.98 kDa (data not shown), indicating that *E. coli* GMP reductase is a tetramer in solution.

Determination of apparent steady-state kinetic constants and initial velocity pattern

The determination of the apparent steady-state kinetic constants was performed using either GMP or NADPH as

This journal is © The Royal Society of Chemistry 2011

View Online

Table 1 Purification protocol of recombinant *E. coli* GMP reductase (2.8 g wet cell paste)

Purification step	Total protein (mg)	Total enzyme activity (U)	Specific activity (U mg^{-1})	Purification fold	Yield (%)
Crude extract	210	89	0.47	1.0	100
Q-Sepharose FF	81	68	0.84	2	76
Sephacryl S-200	47	20	0.44	1.1	23
Mono-Q	45	30	0.66	1.6	34

Downloaded by Pontificia Universidade Catolica do Rio Grande do Sul on 28 February 2011
Published on 07 February 2011 on http://pubs.rsc.org | doi:10.1039/C0MB00245C

the variable substrate, and the data were fitted to eqn (1) (hyperbolic equation), which indicates that the GMP reductase catalyzed reaction follows Michaelis–Menten kinetics.[17] The apparent K_M and V_{max} values for GMP (at 100 μM NADPH fixed concentration) were, respectively, 6.9 (±0.3) μM and 0.065 (±0.001) U mg^{-1}; and the apparent K_M and V_{max} values for NADPH (at 100 μM GMP fixed concentration) were, respectively, 11.1 (±1.2) μM and 0.40 (±0.01) U mg^{-1}. No *E. coli* GMP reductase activity could be detected for varying NADH concentrations (up to 200 μM) in the presence of saturating concentration of GMP. In addition, no enzymatic activity could be detected when, in the presence of saturating levels of NADPH, varying AMP concentrations (up to 1000 μM) were substituted for GMP.

To both determine the true steady-state kinetic parameters and GMP reductase enzyme mechanism, initial velocity as a function of substrate concentration (either GMP or NADPH) was plotted as a linear function of reciprocal of initial velocity against the reciprocal of substrate concentration (double-reciprocal or Lineweaver–Burk plot). The double-reciprocal plots showed a family of lines intersecting to the left of the *y*-axis (Fig. 3), which is consistent with ternary complex formation and a sequential mechanism. Data were plotted in reciprocal form and fitted to the equation for a sequential initial velocity pattern (eqn (2)), yielding the following values for the true steady-state kinetic parameters: k_{cat} = 0.28 (±0.02) s^{-1}, K_{GMP} = 5.5 (±1.0) μM, K_{NADPH} = 14.7 (±2.5) μM, k_{cat}/K_{GMP} = 5.1 (±0.9) × 10^4 M^{-1} s^{-1}, and k_{cat}/K_{NADPH} = 1.9 (±0.3) × 10^4 M^{-1} s^{-1}.

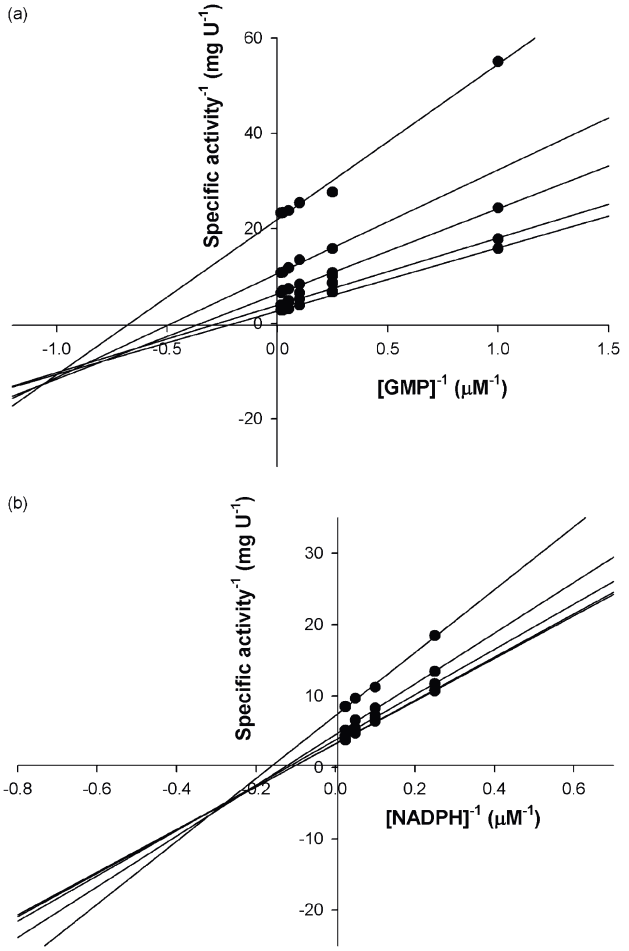

Fig. 3 Intersecting initial velocity patterns for GMP reductase using either GMP (a) or NADPH (b) as the variable substrate. Each curve represents varied-fixed levels of the cosubstrate.

Isothermal titration calorimetry (ITC)

Isothermal titration calorimetry (ITC) experiments were carried out to both determine the relative affinities of substrate(s)/product(s) binding to *E. coli* GMP reductase and provide support for the proposed enzyme mechanism. ITC measurements of ligand equilibrium binding to the enzyme followed the amount of heat generated or consumed upon formation of the binary complex, at constant temperature and pressure. The measure of heat released (exothermic process) upon binding of a ligand provides the binding enthalpy (ΔH)

Table 2 ITC measurements of either GMP or IMP binding to *E. coli* GMP reductase. ΔG = Gibbs free energy changes; ΔS = entropy changes; ΔH = enthalpy changes; K_d = dissociation constants

	Subunit 1	Subunit 2	Subunit 3	Subunit 4
	GMP			
ΔG (kcal mol^{-1})	−5.5 (±8.6)	−6.6 (±5.2)	−6.2 (±9.1)	−5.1 (±6.1)
ΔS (cal mol^{-1} deg^{-1})	−35.1 (±55.4)	133 (±105)	−53 (±78.4)	−4.1 (±4.8)
ΔH (cal mol^{-1})	−16 (±9) × 10^3	3.3 (±3.2) × 10^4	−2.2 (±7.2) × 10^4	−6.3 (±1.1) × 10^3
K_d (μM)	87 (±130)	50 (±39)	15 (±22)	160 (±198)
	IMP			
ΔG (kcal mol^{-1})	−5.6 (±8.5)	−5.3 (±6.6)	−6.9 (±7.5)	−6.2 (±9.0)
ΔS (cal mol^{-1} deg^{-1})	−23 (±34)	100 (±125)	−115 (±125)	−5.4 (±7.8)
ΔH (cal mol^{-1})	−12 (±3) × 10^3	2.4 (±1.9) × 10^4	−1.0 (±2.7) × 10^4	−7.8 (±9.0) × 10^3
K_d (μM)	61 (±92)	142 (±177)	7.8 (±8.5)	26 (±37)

View Online

Downloaded by Pontificia Universidade Catolica do Rio Grande do Sul on 28 February 2011
Published on 07 February 2011 on http://pubs.rsc.org | doi:10.1039/C0MB00245C

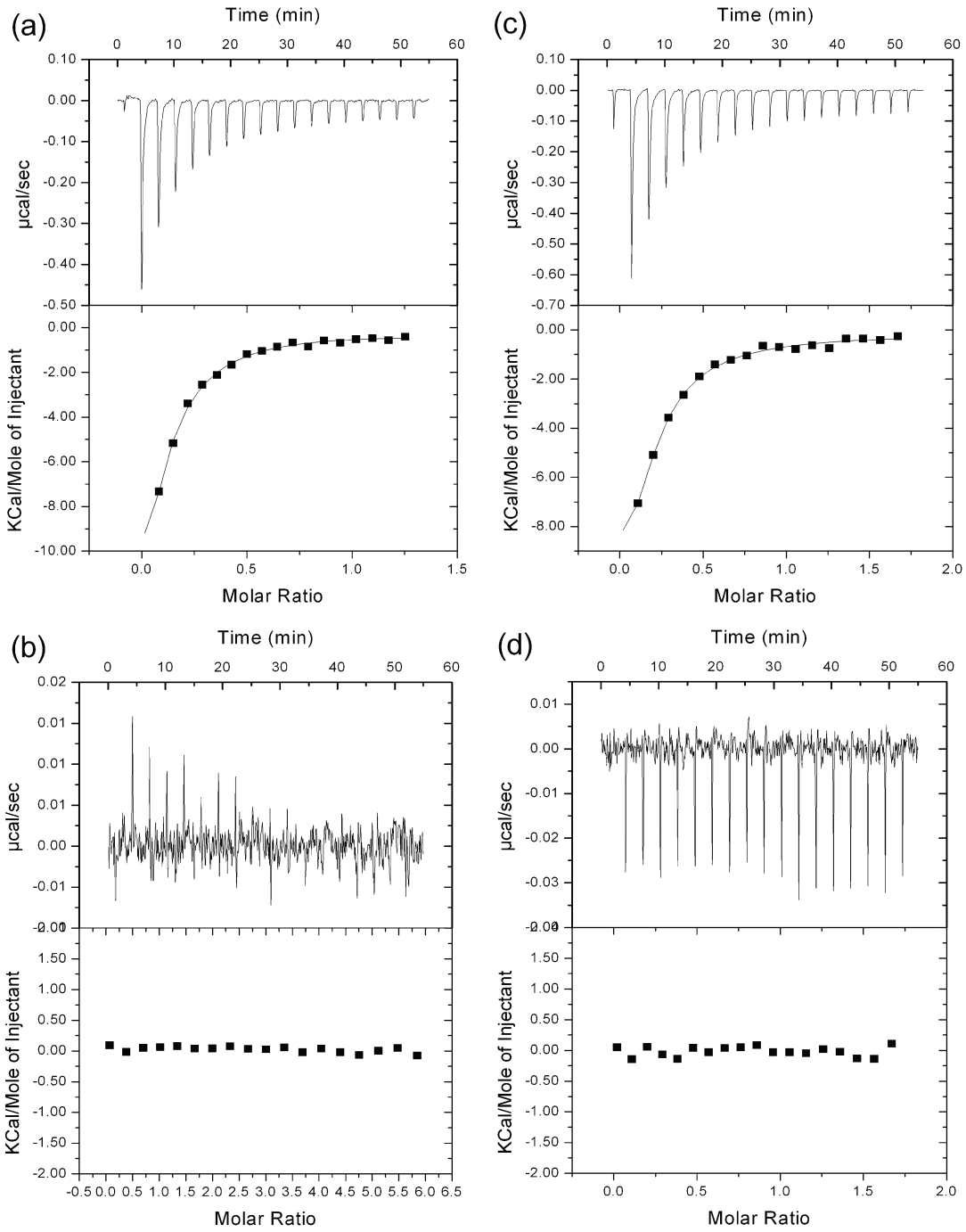

Fig. 4 Isothermal titration calorimetry (ITC) analysis of *E. coli* GMP reductase titration with GMP (a), NADPH (b), IMP (c), and $NADP^+$ (d). The top panels show raw data of the heat pulses resulting from titration of *E. coli* GMP reductase. The bottom panels show the integrated heat pulses, normalized per mole of injectant as a function of the molar ratio (ligand concentration/*E. coli* GMP reductase concentration). These binding curves were best fitted to a sequential binding sites model equation.

of the process, an estimate for the stoichiometry of the interaction (n) and the equilibrium binding constant (K_{eq}). These values allow the Gibbs free energy (ΔG) and the entropy (ΔS) of the process to be calculated.

The ITC data for binding of ligands to *E. coli* GMP reductase are summarized in Table 2. The ITC results showed significant heat changes upon binding of GMP to free *E. coli* GMP reductase enzyme (Fig. 4a), and data fitting to the sequential binding sites model yielded a value of 4 for n, consistent with the quaternary structure determined by gel filtration. This model provides values of ΔH, ΔS, K_{eq} for the binding sites of each subunit. The binding of IMP to the free enzyme also showed significant heat changes (Fig. 4c), and the best fit was also to the sequential binding sites model yielding an n value of 4. No heat change upon the addition of either NADPH or $NADP^+$ to *E. coli* GMP reductase could be detected, suggesting that neither ligand can bind to free enzyme (Fig. 4b and d).

 This journal is © The Royal Society of Chemistry 2011

View Online

Downloaded by Pontificia Universidade Catolica do Rio Grande do Sul on 28 February 2011
Published on 07 February 2011 on http://pubs.rsc.org | doi:10.1039/C0MB00245C

Multiple sequence alignment and *E. coli* GMPR structural analysis

Sequence alignment of GMP reductases from *E. coli* strain K12 (GMPR NC_010473.1) and both human isoforms (hGMPR1 NP_006868.3 and hGMPR2 NP_001002000.1) was performed using the CLUSTALW program.[18] The sequence alignment reveals that the homologues present high similarity (Fig. 5). At the amino acid level, *E. coli* GMP reductase is 65% identical with hGMPR1 and 68% identical with hGMPR2. The proposed catalytic site loop that acts as a lid that closes upon GMP binding is comprised of the conserved residues 179–187[16] (Fig. 5). Based on structural comparison and model building for hGMPR2, it has been suggested that the amino acid residues 129–133 are involved in NADPH binding.[16] These residues are all conserved in *E. coli* GMP reductase (Fig. 5). In addition, the residues involved in GMP binding, which are located in a flexible binding region of hGMPRs,[16] are all conserved in *E. coli* GMP reductase (residues 268–290). Moreover, the N7 of the guanine moiety of GMP makes hydrogen bonds with Met269 and the O6 atom with Ser270 and Gly290, which are all conserved (Fig. 5). It has been shown for hGMPR1 that Ser288 makes hydrogen bonds with N1 and N2 atoms of guanine base.[16] However, this residue is not conserved in *E. coli* GMP reductase, being replaced by Ala288 (Fig. 5). Amino acid residues involved in interactions with the ribose (Asp219 and Arg286) and phosphate (Ser184, Gly221, Gly242, and Gly243) moieties of GMP are all conserved. A disulfide bond between Cys68 and Cys95 side chains has been observed in the crystal structure of hGMPR2, and it has been proposed that it may play a role in stabilization of the tetramer. Interestingly, there are no corresponding residues in *E. coli* GMP reductase indicating that such a disulfide bridge plays no part in stabilization of the tetramer.

The three-dimensional model of *E. coli* GMP reductase was built by restrained-based homology modeling implemented in MODELLER9v1 using the human type 2 GMP reductase structure as a template, as described in more detail in the Experimental procedures section. The three-dimensional model of *E. coli* GMPR indicates high conservation of its tertiary structure as compared to the hGMPR2 structural template, with a RMSD value of 0.61 Å, which is in agreement with the 68% identity at the amino acid level. The model presented no stereochemical parameters violation, as evaluated by PROCHECK package (data not shown), in which 99.2% of *E. coli* GMP reductase amino acids are within allowed regions of the Ramachandran plot. Amino acids involved in GMP binding are almost all conserved in the bacterial homologue (Fig. 5). In addition, there are minor conformational deviations even for the conserved amino acid residues (Fig. 6). The H-bond network of side chains and main chains of these amino acid residues to bound GMP is maintained in both human and *E. coli* GMP reductases. A

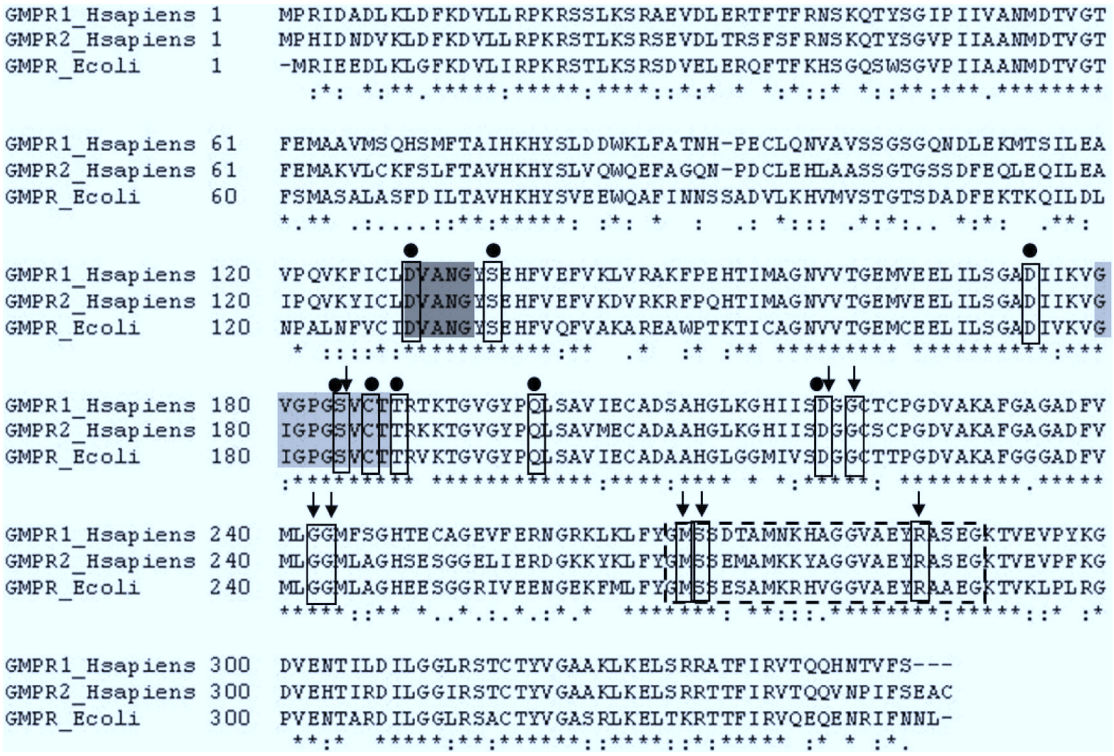

Fig. 5 Multiple sequence alignment of *E. coli* GMP reductase with both human enzymes (GMPR1_Hsapiens and GMPR2_Hsapiens) using the program CLUSTAL W. (*), (:), (.) and (–) indicate, respectively, identity, strong similarity and weak similarity among the residues. The residues in the proposed catalytic site (active site loop that acts as a lid that closes upon GMP binding) were shaded in light gray, the amino acid residues in the proposed NADPH binding site were shaded in dark gray, and amino acid residues in the GMP binding site were boxed by a dashed line. Conserved amino acid residues that are important for catalysis or binding were boxed by a solid line. Black dots above the conserved residue indicate residues involved in catalysis, and black arrows indicate residues involved in substrate binding.

View Online

Downloaded by Pontificia Universidade Catolica do Rio Grande do Sul on 28 February 2011
Published on 07 February 2011 on http://pubs.rsc.org | doi:10.1039/C0MB00245C

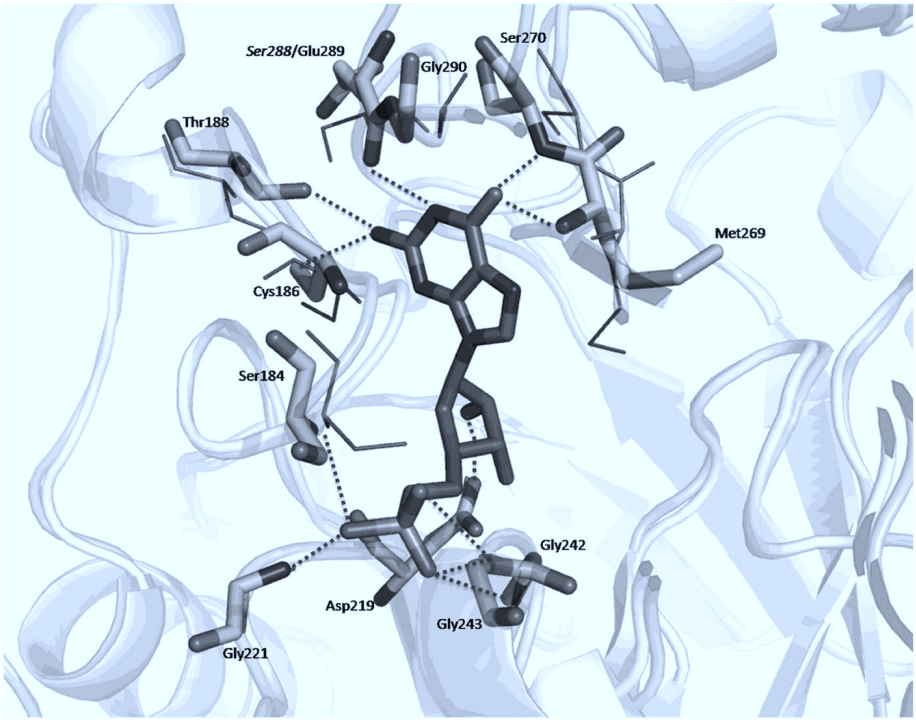

Fig. 6 *E. coli* GMP reductase model superimposed on experimentally solved the human type 2 GMP reductase (hGMPR2) structure. Amino acid residues of *E. coli* GMP reductase involved in GMP binding (light gray) and the GMP molecule (dark gray) are shown as sticks. The corresponding amino acids of the hGMPR2 template are depicted as thin gray sticks. It is noteworthy that Glu289 *E. coli* GMP reductase substitutes for Ser288 in hGMPR2 (italics). H-bonds between amino acid residues of *E. coli* GMP reductase and GMP are shown as dotted lines.

noticeable exception is the Gly290 amino acid residue that is displaced by 1.3 Å away from the substrate binding site in *E. coli* GMP reductase (Fig. 6). Therefore, there is no H-bond between Gly290 and GMP O6 atom since its distance raised from 3.12 Å in the template to 4.4 Å in *E. coli* GMP reductase. The hGMPR2 template structure indicates that the conserved Asp219 residue makes two H-bonds between its carboxyl oxygen atoms and O2′ and O3′ atoms of the GMP ribose moiety. However, our proposed model showed just one H-bond to the O2′ atom of GMP. Although Glu289 *E. coli* GMP reductase substitutes for Ser288 in hGMPR2, there is either no gain or loss of H-bonds between the amino acid side chain at this position and GMP. The H-bond between N1 of the guanine moiety of GMP and the main chain oxygen atom of Glu289 in *E. coli* GMP reductase replaces the same interaction made between the main chain oxygen atom of Ser288 in hGMPR2. The catalytic Cys186 residue that likely plays a critical role in *E. coli* GMP reductase catalysis makes an H-bond to the C2 exocyclic amino group of the guanine moiety of GMP (Fig. 6). Another H-bond is made between Thr188 side chain and the C2 exocyclic amino group of GMP (Fig. 6). Interestingly, according to the PDB coordinates of hGMPR2, there is only one H-bond that is made between Thr188 side chain and the C2 exocyclic amino group of GMP, and Cys186 side chain is H-bonded to Thr188.

pH-rate profiles

To probe for acid–base catalysis, pH dependence studies of k_{cat}, and k_{cat}/K_M for GMP and NADPH were performed. The pH-rate profiles are shown in Fig. 7. The bell-shaped pH-rate data for k_{cat} were fitted to eqn (3), yielding apparent pK values of 6.6 (±0.6) and 9.6 (±1.2) (Fig. 7a), with slopes of +1 for the acidic limb and −1 for the basic limb. These results indicate participation of a single ionizable group in each limb, in which protonation of a group with an apparent pK value of 6.6 and deprotonation of another group with a pK value of 9.6 play critical roles in *E. coli* GMP reductase enzyme catalysis. The pH-rate data for of k_{cat}/K_{GMP} were fitted to eqn (4) and indicate that both protonation of two groups with apparent pK values of 7.1 (±0.8) and deprotonation of two groups with apparent pK values of 8.6 (±1.1) (Fig. 7b) are required for binding of GMP. The data of the pH-rate profile for k_{cat}/K_{NADPH} were fitted to eqn (5), which suggests that protonation of two groups with apparent pK values of 6.2 (±1.0) abolish NADPH binding to *E. coli* GMP reductase (Fig. 7c).

Energy of activation

The energy of activation for the enzyme-catalyzed chemical reaction was assessed by measuring the dependence of k_{cat} on temperature (Fig. 8). These data were fitted to eqn (6), yielding a value of 4.4 kcal mol^{-1}, which represents the minimal amount of energy necessary to initiate the chemical reaction catalyzed by *E. coli* GMP reductase. The linearity of the Arrhenius plot (Fig. 8) also suggests that there is no change in the rate-limiting step over the temperature range utilized in the assay.

Deuterium kinetic isotope effects and proton inventory

To probe for rate-limiting steps and determine the stereospecificity of hydride transfer, measurements of primary

 This journal is © The Royal Society of Chemistry 2011

View Online

Downloaded by Pontificia Universidade Catolica do Rio Grande do Sul on 28 February 2011
Published on 07 February 2011 on http://pubs.rsc.org | doi:10.1039/C0MB00245C

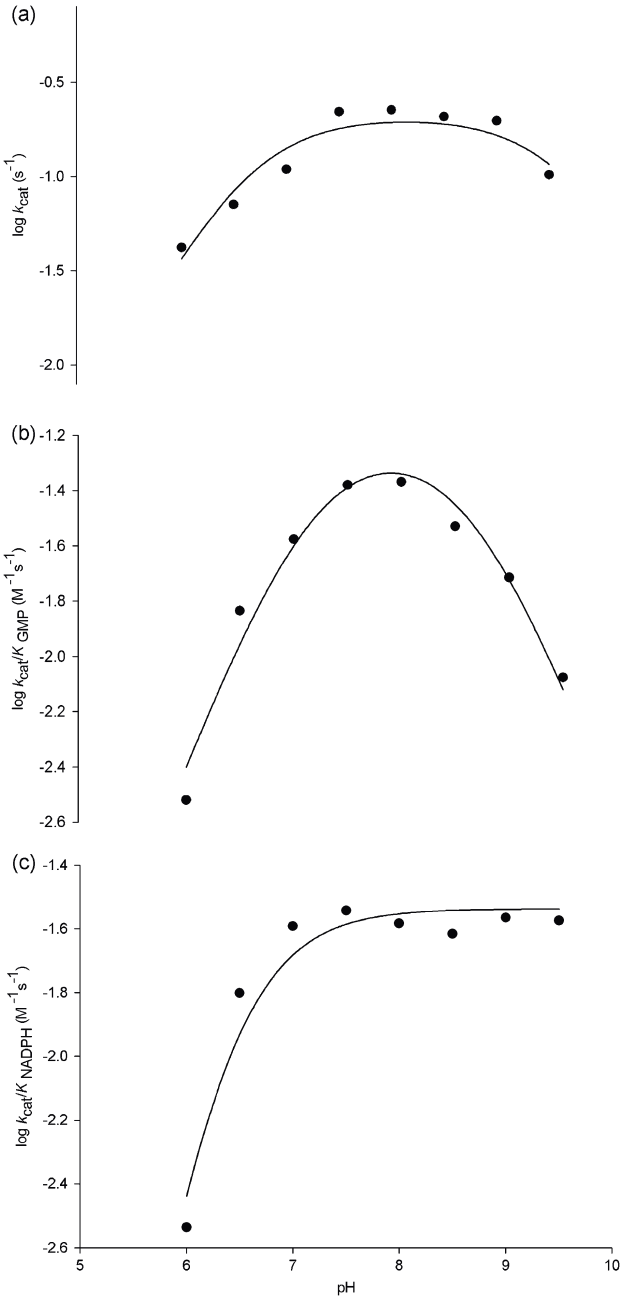

Fig. 7 Dependence of kinetic parameters on pH. (a) pH dependence of log k_{cat} data were fitted to eqn (3); (b) log k_{cat}/K_{GMP} data were fitted to eqn (4); (c) pH dependence of log k_{cat}/K_{NADPH} data were fitted to eqn (5).

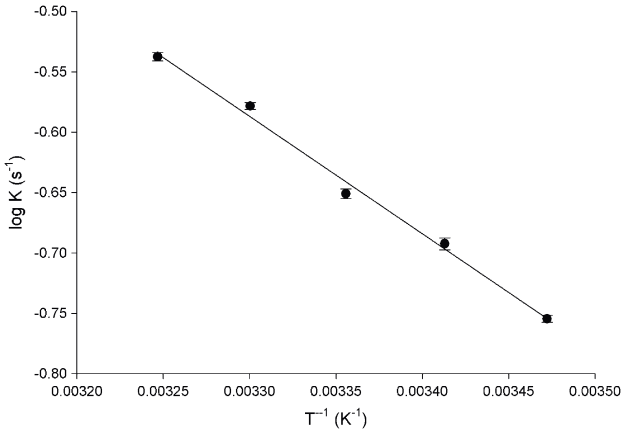

Fig. 8 Temperature dependence of log k_{cat}. Saturating concentrations of NADPH and GMP substrates were employed to measure the maximum velocity as a function of temperature ranging from 15 to 35 °C. The data were fitted to eqn (6). The linearity of the Arrhenius plot suggests that there is no change in the rate-limiting step over the temperature range utilized in the assay.

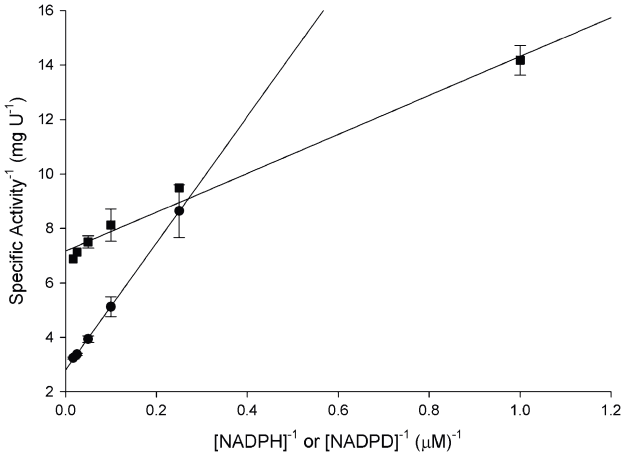

Fig. 9 Primary deuterium kinetic isotope effects using either NADPH (●) or NADPD (■) as the variable substrate in the presence of saturating concentration of GMP (100 μM). The data were fitted to eqn (7).

deuterium kinetic isotope effects were carried out (Fig. 9). The data were fitted to eqn (7) for kinetic isotope effects on both V and V/K, yielding values of 2.50 (±0.04) for $^{D}V_{NADPH}$ and 0.40 (±0.04) for $^{D}V/K_{NADPH}$ (Table 3). The corresponding values for GMP were 1.05 (± 0.06) for $^{D}V_{GMP}$ and 1.03 (± 0.07) for $^{D}V/K_{GMP}$ (Table 3).

To evaluate the contribution of proton-transfer from the solvent to the GMP reductase catalyzed reaction, solvent kinetic isotope effects were determined and the data fitted to eqn (7). The following values were found for the solvent kinetic isotope effects (Table 3): $^{D_2O}V_{NADPH}$ = 0.99 (±0.03)

Table 3 Kinetic isotope effects for *E. coli* GMP reductase[a]

Parameter	Isotope effect
$^{D}V/K_{NADPH}$	0.40 ± 0.04
$^{D}V_{NADPH}$	2.50 ± 0.04
$^{D}V/K_{GMP}$	1.03 ± 0.07
$^{D}V_{GMP}$	1.05 ± 0.06
$^{D_2O}V/K_{NADPH}$	0.67 ± 0.09
$^{D_2O}V_{NADPH}$	0.99 ± 0.03
$^{D_2O}V/K_{GMP}$	0.82 ± 0.03
$^{D_2O}V_{GMP}$	1.30 ± 0.01
$^{D_2O}V/K_{NADPD}$	1.50 ± 0.17
$^{D_2O}V_{NADPD}$	1.00 ± 0.02
$^{D}K_{eq}$	0.82

[a] Value ± standard error obtained upon data fitting to the appropriate equations.

View Online

Downloaded by Pontificia Universidade Catolica do Rio Grande do Sul on 28 February 2011
Published on 07 February 2011 on http://pubs.rsc.org | doi:10.1039/C0MB00245C

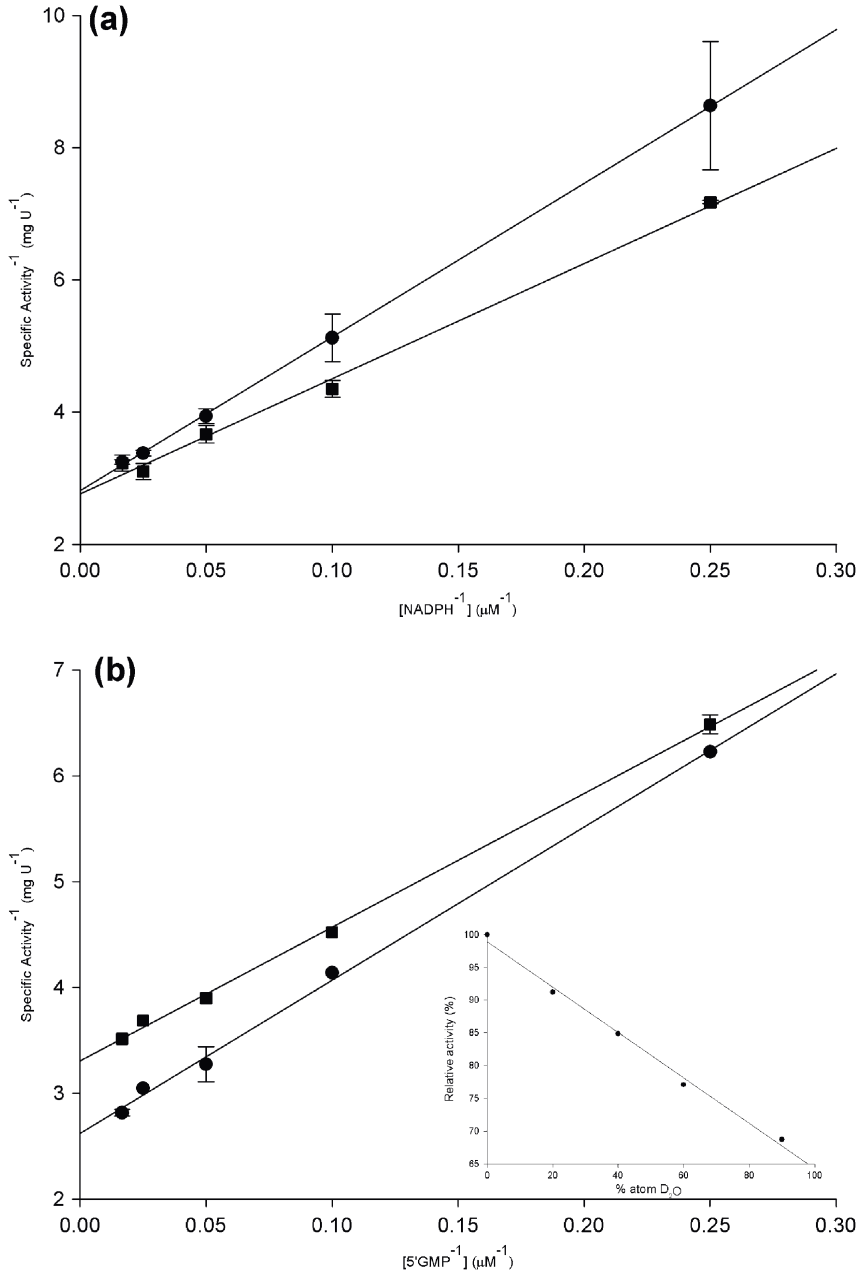

Fig. 10 Solvent isotope effects for GMP reductase. (a) NADPH was used as the variable substrate (4–60 μM), with a saturating concentration of GMP (100 μM). (b) GMP was used as the variable substrate (4–60 μM), with a saturating concentration of NADPH (100 μM). Both reactions mix contained either 0 (●) or 90 (■) atom% D_2O. The inset of (b) represents the proton inventory (0, 20, 40, 60, and 90 atom% D_2O) measuring GMP reductase enzyme activity with both substrates at saturating concentrations (100 μM).

and $^{D_2O}V/K_{NADPH}$ = 0.67 (±0.09) (Fig. 10a), and $^{D_2O}V_{GMP}$ = 1.30 (±0.01) and $^{D_2O}V/K_{GMP}$ = 0.82 (±0.03) (Fig. 10b). In an attempt to determine the number of protons transferred during the solvent isotope-sensitive step, a proton inventory experiment was conducted. A linear relationship between V and the mole fraction of D_2O for GMP reductase (Fig. 10b—inset) was found, suggesting that a single proton is transferred during this step.

Multiple isotope effects are capable of discriminating if two different isotopic substitutions affect the same or distinct chemical steps. Accordingly, solvent kinetic isotope effects were measured using NADPD as the varied substrate. Isotope effect values on $^{D_2O}V_{NADPD}$ and $^{D_2O}V/K_{NADPD}$ were, respectively, 1.00 (±0.02) and 1.50 (±0.17) (Fig. 11; Table 3). The isotope effect on the equilibrium constant, $^{D}K_{eq}$, was determined in order to assess whether the deuterium substitution could affect the internal equilibrium of the reaction. A value of 0.82 was determined for the equilibrium isotope effect ($^{D}K_{eq}$; Table 3).

Pre-steady-state kinetics

In an attempt to determine whether product release contributes to some extent to the rate limiting step, pre-steady-state

 This journal is © The Royal Society of Chemistry 2011

View Online

Downloaded by Pontificia Universidade Catolica do Rio Grande do Sul on 28 February 2011
Published on 07 February 2011 on http://pubs.rsc.org | doi:10.1039/C0MB00245C

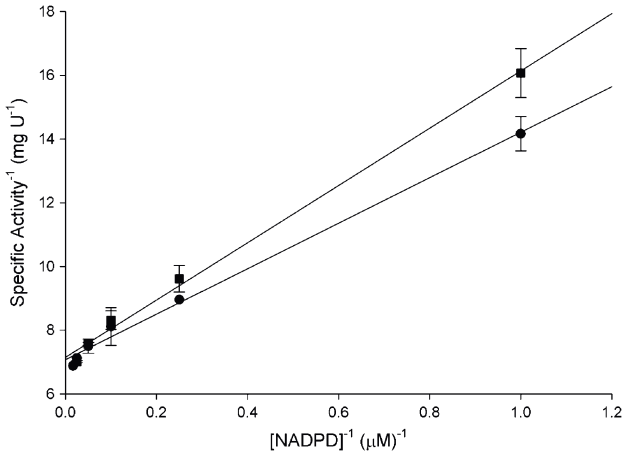

Fig. 11 Multiple kinetic isotope effects using NADPD as the variable substrate in the presence of saturating concentration of GMP (100 μM) and either 0 (●) or 80 (■) atom% D_2O. The data were fitted to eqn (7).

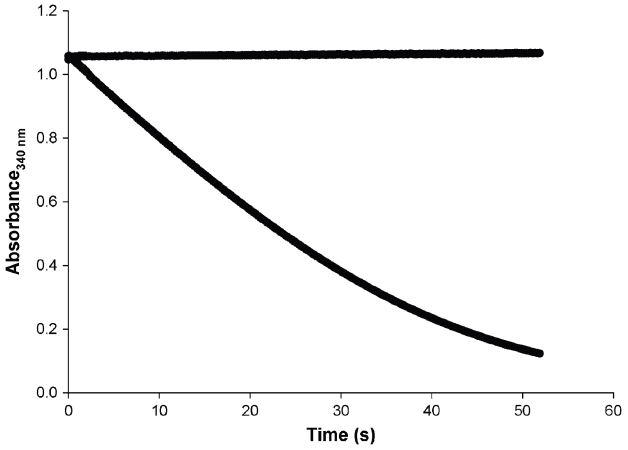

Fig. 12 Representative stopped-flow trace for product formation, measuring the decrease in absorbance at 340 nm upon conversion of NADPH to $NADP^+$ catalyzed by 10 μM of recombinant *E. coli* GMP reductase (mixing chamber concentration) in the presence of GMP. The data were fitted to eqn (10) for a single exponential decay, yielding a value of 0.204 s^{-1} for the apparent first-order constant of product formation. The top stopped-flow trace represents the control experiment in the absence of the GMP substrate.

analysis of the reaction catalyzed was performed. Fitting the pre-steady-state data to eqn (10), which describes a single exponential decay, yielded a value of 0.204 (±0.002) s^{-1} for the apparent first-order rate constant (Fig. 12). This result is in agreement with the value of 0.28 (±0.02) s^{-1} for the catalytic rate constant (k_{cat}) determined by initial velocity study measurements.

Discussion

Amplification, cloning, expression and purification of recombinant *E. coli* GMP reductase

The *guaC* gene was successfully amplified from the *E. coli* genome, cloned into the pCR-Blunt vector, and subcloned into the pET-23a(+) expression vector. The automatic DNA sequencing confirmed the integrity of the gene and the absence of mutations. *E. coli* GMP reductase was expressed after 24 h of cell growth in the absence of IPTG induction. The pET expression system makes use of a powerful T7 polymerase, under control of the IPTG-inducible *lacUV5* promoter to transcribe genes of interest, which are positioned downstream of the bacteriophage T7 late promoter.[19] Expression of recombinant GMP reductase showed that even in the absence of the inducer, high levels of protein production could be obtained in the stationary phase, as has been previously reported for other enzymes.[20–22] It has been proposed that uninduced expression of *lac*-controlled genes occurs when cells approach the stationary phase in complex medium and that cAMP, acetate and low pH are required to produce high level expression in the absence of IPTG induction, which perhaps is part of a general response to carbon-limiting conditions.[23] Nevertheless, more recently, it has been shown that unintended induction in the pET system is due to the presence of as little as 0.0001% of lactose in the medium.[24] The recombinant *E. coli* GMP reductase was purified to homogeneity by a three-step purification protocol using standard anionic exchange and size exclusion columns with 33% of protein yield.

Quaternary structure analysis of *E. coli* GMP reductase

The results of mass spectrometry analysis combined with the amino acid sequencing demonstrated, unequivocally, that the homogeneous protein is, indeed, recombinant *E. coli* GMP reductase. The gel filtration chromatography showed that the enzyme from *E. coli* has the same tetrameric quaternary structure of hGMPR2, demonstrated by X-ray diffraction.[16]

Determination of apparent steady-state kinetic constants and initial velocity pattern

The results of the apparent steady-state kinetic data for *E. coli* GMP reductase indicate a K_M value for GMP of 6.9 μM, which is 2.5-fold lower than that for hGMPR2 (17.4 μM),[2] and 3-fold lower than the enzyme from *L. donovani* (21.2 μM).[9] The same pattern occurs for NADPH, with a K_M value of 11.1 μM, which is 2.3-fold lower than that for hGMPR2 (26.6 μM).[2] As for its human counterparts, *E. coli* GMP reductase cannot catalyze conversion of GMP to IMP using NADH as the hydride donor up to 200 μM concentration (data not shown).

Lineweaver–Burk analysis (Fig. 3) suggests that ping-pong and rapid equilibrium ordered mechanisms can be ruled out for *E. coli* GMP reductase. The former mechanism gives double reciprocal plots displaying parallel lines and the latter a family of lines intersecting on the *y*-axis. These data are consistent with ternary complex formation and a sequential mechanism. A sequential mechanism was also reported for hGMPR1[11] and hGMPR2.[2]

It has been shown that the true K_M values for erythrocyte hGMPR1 are 2.6 μM for GMP and 16.9 μM for NADPH,[11] which are in the same concentration range as *E. coli* GMP reductase true steady-state kinetic parameters. These results suggest that *E. coli* GMP reductase possesses a similar overall

View Online

Downloaded by Pontificia Universidade Catolica do Rio Grande do Sul on 28 February 2011
Published on 07 February 2011 on http://pubs.rsc.org | doi:10.1039/C0MB00245C

dissociation constant for both substrates when compared to hGMPR1. However, the erythrocyte human enzyme presents a bimodal GMP substrate saturation curve,[11] which is usually attributed to the existence of independent isoenzymes with different kinetic constants or to a single multisubunit enzyme with multiple sites that can interact in a negatively cooperative manner.[25] Deng and co-workers[2] identified the hGMPR2 isoenzyme, making the bimodal substrate-saturation kinetic found in hGMPR likely to be a result of a mixture of both isoenzymes. At any rate, a sequential addition of substrates to form a ternary complex has also been proposed for hGMPR2 enzyme.[2]

Isothermal titration calorimetry

ITC is an important and well-established technique for the study of thermodynamics of macromolecular interactions, and is unique in that it is capable of measuring simultaneously the association and thermodynamic constants of binding.[26] Binding experiments using ITC combined with the initial velocity study demonstrated that the reaction catalyzed by *E. coli* GMP reductase follows an ordered bi–bi kinetic mechanism, in which GMP is the first substrate to bind to free enzyme, followed by the binding of NADPH to form the ternary complex capable of undergoing catalysis; and $NADP^+$ is the first product to dissociate from the enzyme, followed by the dissociation of IMP (Fig. 13). This mechanism is in agreement with both human GMP reductases, for which a sequential kinetic mechanism has been reported.[2,11] Notwithstanding, the results reported here provide, to the best of our knowledge, the first experimental evidence for both order of addition of substrate and release of products.

The ITC measurements of GMP binding provided dissociation constant values (K_d), one for each subunit, where $K_{d1} > K_{d2} > K_{d3}$, suggesting a positive homotropic cooperativity, since the binding of one molecule of GMP increases the affinity for the next molecule which will bind to the next subunit. The K_{d4} value is higher than the others, indicating a lower affinity for the last subunit to bind GMP. Interestingly, this finding is consistent with the crystal structure of hGMPR2, as no GMP binding could be observed for one of the subunits of this enzyme.[16] However, the large errors do not warrant to ascertain whether or not there is cooperativity on GMP binding to *E. coli* GMP reductase. The ΔG values for all four subunits are negative, which demonstrate that GMP binding to *E. coli* GMP reductase is a thermodynamically favorable process. The thermodynamic analysis revealed different types of interactions between the ligand and the enzyme subunits, ranging from favorable hydrogen bonds and/or van der Waals interactions (negative ΔH), release of "bound" water molecules to the bulk solvent (positive ΔS) to conformational changes in either or both of the molecules (negative ΔS).[27] As can be seen in Table 2, with the exception of subunit 2, the analyses of ΔH and ΔS reveal that the binding of GMP is coupled with favorable hydrogen bonds (negative ΔH) and conformational changes (negative ΔS).[28] This finding appears to be consistent with the hGMPR2 structure,[16] in which GMP was located on the top of the α/β barrel surrounded by a hydrophilic surface formed by the active site loop and the flexible binding loop that would close upon GMP binding to the enzyme.

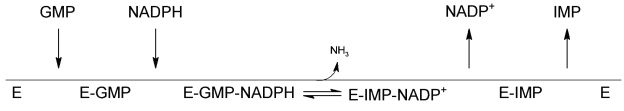

Fig. 13 Proposed enzyme mechanism for *E. coli* GMP reductase.

The IMP binding to *E. coli* GMP reductase yielded four different K_d values (Table 2). However, the large errors do not allow us to propose that there is either positive or negative cooperativity among the subunits upon IMP binding. The analysis of the Gibbs free energy revealed that the binding of IMP is thermodynamically favorable for all subunits of *E. coli* GMP reductase (negative ΔG), and the analysis of ΔH and ΔS for IMP follows a similar pattern as observed for GMP. The determination of the crystal structure of *E. coli* GMP reductase in complex with IMP may shed light on these thermodynamic features.

The rather large standard errors (Table 2) are a direct consequence of the shape of the binding isotherm (*C* value), which will dictate how accurately the thermodynamics parameters can be determined.[27] The shape of the binding is dependent on K_d and the concentration of the macromolecule. The latter is limited by the need to obtain large quantities and/or solubility. Another consideration is that for the experimental set-up it is important to obtain an isotherm that provides maximum data points for the fitting process,[27] and the loss of the plateau in the beginning of the titration curve might have contributed to the large standard errors. We were unable to determine the initial points due to rather small ΔH values. At any rate, the ITC data provided clear-cut experimental evidence of GMP and IMP binding to free *E. coli* GMP reductase enzyme (Fig. 4a and c) that allowed the proposal of an ordered bi–bi kinetic mechanism with GMP binding first (Fig. 13). In addition, the ITC data provided thermodynamic signatures of non-covalent interactions between *E. coli* GMP reductase and either GMP or IMP.

pH-rate profiles

The Cys186 amino acid side chain has been shown to play a key role in catalysis for hGMPR2 since the Cys186Ala mutant displayed less than 5% activity as compared to wild-type enzyme.[16] The pH dependence of k_{cat} and sequence alignment analyses suggest that the conserved Cys186 is likely the residue with an apparent p*K* value of 9.6 that plays a critical role in *E. coli* GMP reductase catalysis. The cysteine thiol group usually ionizes at slightly alkaline pH values, and the resulting thiolate anion is the reactive species that acts as a nucleophile, which is one of the most reactive functional groups found in proteins.[29] It is possible that the Cys186 side chain, which has been shown to interact with GMP in the crystal structure of hGMPR2,[16] interacts with the exocyclic amino group bound to C2 of the guanine moiety of GMP thereby facilitating both hydride transfer to C2 and the amino leaving group. In addition, the proposed model of *E. coli* GMP reductase indicates that this residue makes an H-bond to the C2 exocyclic amino group of the guanine moiety of GMP (Fig. 6). Notwithstanding, site-directed mutagenesis studies

 This journal is © The Royal Society of Chemistry 2011

View Online

Downloaded by Pontificia Universidade Catolica do Rio Grande do Sul on 28 February 2011
Published on 07 February 2011 on http://pubs.rsc.org | doi:10.1039/C0MB00245C

are in progress to confirm the role of Cys186, if any, in *E. coli* GMP reductase enzyme catalysis. The bell-shaped pH profile for k_{cat} (Fig. 7a) also showed participation of a single ionizable group with an apparent pK value of 6.6 that has to be deprotonated for catalysis. Sequence alignment showed conservation of Asp129 in *E. coli* GMP reductase (Fig. 7) that has been shown to be located in the active site loop in hGMPR2.[16] Although the pK value of the β-carboxyl group of Aspartate residues are usually in the 3.9–4.0 range, it is not unlikely that this pK value may be displaced by a neighbouring chemical group. However, assigning a definite catalytic role to Asp129 in *E. coli* GMP reductase is not warranted and site-directed mutagenesis studies should be carried out. Although the apparent pK value of 6.6 that plays a role in catalysis could tentatively be ascribed to the imidazole side chain of a Histidine residue (pK usually in the 6.0–7.0 range), His278 is located in the GMP binding site of *E. coli* GMP reductase whereas it is not present in hGMPR2 (Fig. 7).

The pH-rate data for of k_{cat}/K_{GMP} indicate that both protonation of two groups with apparent pK values of 7.1 and deprotonation of two groups with apparent pK values of 8.6 (Fig. 7b) are required for GMP binding. These dissociation constants can be in the ligand and the other in the enzyme, or both can be in one or the other. The crystal structure of hGMPR2 in complex with GMP demonstrated that this substrate is surrounded by a hydrophilic surface formed by the active site loop (residues 179–187 in hGMPR2) and the flexible GMP binding region (residues 268–290 in hGMPR2).[16] Sequence alignment of GMP reductases (Fig. 5) shows a relatively good conservation of these two regions in *E. coli* GMP reductase (active site loop: residues 179–187; GMP binding region: 268–290). The pK value for the N7 atom of the guanine moiety of GMP is 3.6, and the ribose 2′,3′-diol only loses a proton above pH 12. The guanine base becomes protonated on one of the ring nitrogens rather than on the exocyclic amino group since this does not interfere with delocalization of the NH_2 electron lone pair into the aromatic system. In the case of monoesters, the phosphate group of GMP loses one proton at pH 1 and a second proton at pH 7. The proximity of negative charge on the phosphate residues has a secondary effect, making the ring nitrogens more basic ($\Delta pK \approx +0.4$) and the amine protons less acidic ($\Delta pK \approx +0.6$). It is thus likely that the pH-rate profile does not reflect any ionization of the guanine moiety of GMP. On the other hand, it is possible that the apparent pK values reflect change in ionization of His278 in the GMP binding site, and change in ionization of the phosphate group of GMP and, for instance, Asp219 that makes H-bonds with the ribose hydroxyl groups of the pentose.

The pH-rate profile for k_{cat}/K_{NADPH} indicated that protonation of two groups with apparent pK values of 6.2 abolish NADPH binding to *E. coli* GMP reductase (Fig. 7c). Although there was no diffraction pattern to allow identification of the NADPH binding site in hGMPR2, structural comparison and model building has been employed to suggest that the amino acid residues 129–133 are involved in NADPH binding.[16] These residues are conserved in *E. coli* GMP reductase (Fig. 5). The adenine-C2′-ribose phosphate group has a pK value of 6.1. It is thus tempting to suggest that protonation of NADPH phosphate and the putative Asp129 residue located in the NADPH binding site can account for the k_{cat}/K_{NADPH} pH-rate profile.

Deuterium kinetic isotope effects and proton inventory

Measurements of kinetic isotope effects in enzyme catalyzed reactions aim at examining the contribution of proton transfer(s) to rate-limiting step(s). However, the maximal velocity may be dependent on several rate-contributing or partially rate-limiting steps instead of one rate-determining step.[30]

Isotope effects on V report on events following the ternary complex formation capable of undergoing catalysis (fully loaded enzyme), which include the chemical steps, possible enzyme conformational changes, and product release (leading to regeneration of free enzyme). Isotope effects on V/K report on steps in the reaction mechanism from binding of the isotopically labeled substrate to the first irreversible step, usually considered to be the release of the first product (that is, all rate constants from reactant binding until the first irreversible step).[30] Any substrate can be varied; it does not need to be the labeled one, but one obtains $^{D}V/K$ effect for the varied substrate rather than for the labeled one. Although the apparent classical limit for primary deuterium kinetic isotope effects on V is approximately 8, values as low as 2 have sometimes been accepted as evidence of a rate-determining step.[30,31] For reactions involving NAD(P)H oxidation, primary deuterium isotope effects ranging from 1 to 3 have been found.[32] The magnitude of primary deuterium isotope effect depends on the chemical nature of the transition state.[33] This isotope effect reaches a maximum value when the hydrogen is symmetrically placed between the donor atom from which cleavage occurs and the acceptor atom to which a new bond is formed, and decreases for reactant- or product-like transition states. The value of 2.5 for the observed primary deuterium kinetic isotope effect on V for *E. coli* GMP reductase using either NADPH or [4*S*-^{2}H]-NADPH ($^{D}V_{NADPH}$) as a variable substrate indicates that hydride transfer is involved in a rate-limiting step and that the transition state may be either substrate- (early) or product-like (late). However, the symmetry of the transition state can only be inferred from the magnitude of a deuterium kinetic isotope effect if it is for the specific step in an enzymatically catalyzed reaction at which the isotopically substituted bond is broken by passing through a single transition state (that is, the intrinsic kinetic isotope effect). Enzyme-catalyzed chemical reactions proceed through many steps and the rate constants for several steps are usually consequential to the composite rate constant for the overall reaction, consequently the observed deuterium kinetic isotope effect is less than or equal to the intrinsic deuterium isotope effect for the step in which the hydrogen is transferred. In any case, the observed primary deuterium kinetic isotope effect on V for *E. coli* GMP reductase indicates that hydride transfer is from C4-*proS* hydrogen of NADPH and that it is partially rate-limiting. On the other hand, the inverse primary deuterium kinetic effect on V/K for NADPH ($^{D}V/K_{NADPH} = 0.4$) is somewhat puzzling. Incidentally, there have been numerous reports of inverse isotope effects on V/K of unknown origin.[34,35]

View Online

Downloaded by Pontificia Universidade Catolica do Rio Grande do Sul on 28 February 2011
Published on 07 February 2011 on http://pubs.rsc.org | doi:10.1039/C0MB00245C

The expression of deuterium kinetic isotope effect on V/K includes the intrinsic isotope effect, commitment factors (forward and reverse) and equilibrium isotope effect.[33] An equilibrium isotope effect may be invoked to account for the inverse effect on V/K, providing that the reverse commitment factor is large and the forward commitment factor is small. The inverse deuterium isotope effect on the equilibrium constant ($^{D}K_{eq}$ = 0.82) suggests that the deuterated product is more stiffly bonded than the deuterated substrate[36] and the internal equilibrium might dominate the observed kinetic isotope effect. The inverse isotope effect indicates that once the hydride is transferred it becomes more tightly bonded to the corresponding product (IMP) when compared to the substrate. The magnitude of this isotope effect is a direct consequence of the difference in the bonds of the substrate and product, with deuterium becoming enriched in the stiffest bond and the hydrogen in the looser one (deuterium accumulates where binding is tighter).[37] In addition, isotope effects on V/K are a combination of binding and catalytic events. Binding isotope effects can contribute in the opposite direction of kinetic isotope effects that arise from transition state chemistry. An inverse binding isotope effect may arise when binding of the molecule containing the heavier isotope atom (NADPD) is increased as bonds to the isotopic label are tighter in the bound complex. Although it is conceivable that the inverse $^{D}V/K_{NADPH}$ value reflects an inverse binding isotope effect, it cannot be experimentally assessed as NADPH (enzyme mechanism proposed here) binds to the *E. coli* GMP reductase:GMP binary complex to form the catalytic competent ternary complex. Accordingly, the inverse $^{D}V/K_{NADPH}$ value is likely due to the inverse deuterium isotope effect on the equilibrium constant. Isotope effects can provide further experimental evidence for a specific enzyme mechanism. In the case of an ordered mechanism, the V/K for the first substrate (GMP) to bind (at saturating concentrations of the second substrate: NADPH) is the on-rate for the reactant binding to enzyme, a non-isotope sensitive step.[33] The value of 1.03 ($\pm$ 0.07) for $^{D}V/K_{GMP}$ (Table 3) provides further support for an ordered enzyme mechanism as suggested by the initial velocity pattern and ITC data.

To evaluate the contribution of proton transfer from solvent to a rate-limiting step, measurements of solvent isotope effects on V and V/K were carried out. As rule of thumb, deuterium accumulates where binding is tighter (that is, fractionation factor is larger than one). Transition state proton contributes the reciprocal of its respective fractionation factor to the solvent isotope effect, whereas the contribution of a reactant state proton to the solvent isotope effect is equal to its fractionation factor.[32] Reactant state fractionation by enzyme cysteine thiol groups (S–H group of cysteine) can make large inverse contributions to solvent isotope effects.[32,33] It is thus conceivable that the value of 0.82 for $^{D_2O}V/K_{GMP}$ reflects participation of Cys186 of free enzyme, which has been shown to interact with GMP in the hGMPR2 crystal structure,[16] and the value of 0.67 for $^{D_2O}V/K_{NADPH}$ reflects an inverse contribution of conserved Cys127 of free enzyme, located near the NADPH binding site of *E. coli* GMP reductase (Fig. 5). The value of 0.99 for $^{D_2O}V_{NADPH}$ suggests no participation of the proton solvent in catalysis. On the other hand, solvent proton transfer appears to play a modest role in catalysis since a value of 1.30 was found for $^{D_2O}V_{GMP}$. In addition, proton inventory data (Fig. 10b—inset) suggest that this modest solvent kinetic isotope effect arises from a single protonic site. The difference found between the primary deuterium and solvent kinetic isotope effects suggests that the hydride and proton transfer may occur in distinct reaction steps, as found in other NADPH-dependent reductive reactions.[34] Nevertheless, it is not possible to ascertain whether or not hydride transfer and protonation steps occur in a single transition state (concerted mechanism) or in distinct transition states (stepwise mechanism) based solely on primary and solvent isotope effects.

Multiple isotope effects (double isotope effects) allow us to determine whether two different isotopic substitutions affect the same (concerted) or different (stepwise) chemical steps.[38] This method uses the normal effect of deuterium to slow down one step of a reaction mechanism while observing changes in the expression of another isotope effect,[38] the effects in question being the protonation and the hydride transfer. If the protonation and hydride transfer occur in the same transition state, the solvent isotope effect will be larger or unchanged with the deuterium substitution (NADPD) when compared with NADPH. However, if the effects take place in different steps, the solvent isotope effect will decrease with NADPD, once the hydride transfer will become more rate-limiting.[34,35,38] As can be seen in Table 3, the results of the multiple isotope effects showed similar values for $^{D_2O}V_{NADPD}$ (1.00) and $^{D_2O}V_{NADPH}$ (0.99), suggesting that hydride transfer and solvent proton transfer steps take place in the same transition state (concerted mechanism). In addition, the value for the solvent isotope effect on V/K with NADPD (1.50) is larger than with NADPH (0.67), thereby lending support to a concerted mechanism.

Pre-steady-state kinetics

In the study of the transient phase of enzyme reactions, the data obtained are generally expressed by a single exponential curve for the first order reaction.[39] The analysis of the data allows us to determine the apparent first order rate constant, which was in the same range as the first order in the steady-state kinetics. The observation of burst during a time course in the transient phase is evidence of a significant build-up of product formation along the reaction pathway.[39] If a burst is observed during the transient phase, and the concentration of $NADP^+$ produced is approximately equal to the initial *E. coli* GMP reductase subunit concentration, it would indicate that the chemical step of the reaction is much faster than the release of the first product ($NADP^+$). As there is no burst of $NADP^+$ formation (Fig. 12), the stopped-flow result demonstrates that product release does not contribute to the rate-limiting step of the chemical reaction catalyzed by *E. coli* GMP reductase.

Conclusion

A rational inhibitor design relies on mechanistic and structural information on the target enzyme. Enzyme inhibitors make up roughly 25% of the drugs marketed in United States.[40] Enzymes catalyze multistep chemical reactions to achieve rate

 This journal is © The Royal Society of Chemistry 2011

View Online

Downloaded by Pontificia Universidade Catolica do Rio Grande do Sul on 28 February 2011
Published on 07 February 2011 on http://pubs.rsc.org | doi:10.1039/C0MB00245C

accelerations by stabilization of transition state structure(s).[40] Accordingly, mechanistic analysis should always be a top priority for enzyme-targeted drug programs aiming at the rational design of potent enzyme inhibitors. Moreover, ITC has been used as an important technique for the direct determination of thermodynamic and kinetic parameters of enzymatic reactions.[41] The recognition of the limitations of high-throughput screening approaches in the discovery of candidate drugs has rekindled interest in rational design methods.[42] Understanding the mode of action of *E. coli* GMP reductase will inform us on how to better design inhibitors targeting this enzyme. In addition, understanding the mode of action of an enzyme can be used to inform functional annotation of newly determined sequences and structures, to select appropriate enzyme scaffolds for engineering new functions, and to refine definitions in the current EC classifications.[43] The elucidation of the mode of action of *E. coli* GMP reductase and its availability in recombinant form may also provide a tool for determination of substrate specificity of cyclic nucleotide phosphodiesterases (PDEs). PDEs belong to a superfamily of proteins with medical relevance that play a major role in cell signaling by catalyzing the hydrolysis of cyclic AMP (cAMP) and cyclic GMP (cGMP).[44] PDE enzymes are distinguished by their substrate specificity. The PDE activity cannot be directly assayed, being necessary to couple an accessory enzyme. As recombinant *E. coli* GMP reductase is specific for GMP, it may be employed to determine the substrate specificity of PDE enzymes. Among the 11 families of PDEs, only PDE 5, PDE 6 and PDE 9 are specific for cGMP, which are targets for, respectively, treatment of erectile dysfunction (sildenafil), visual alterations, and behavioral state regulations and learning.[45] The results here presented may also help chemical biologists to design function-based chemical compounds to carry out either loss-of-function (inhibitors) or gain-of-function (activators) experiments to reveal the biological role of GMP reductase in the context of whole *E. coli* cells.[46] It is also hoped that the results presented here may be useful to understand the role that GMP reductase plays in the *E. coli* salvage pathway.

Experimental procedures

Materials

All chemicals were of analytical or reagent grade and were used without further purification, unless stated otherwise. 5′GMP, NADPH, IMP, and $NADP^+$ along with lysozyme and streptomycin sulfate were purchased from Sigma-Aldrich. Deuterium oxide (99.9 atom% D_2O) was from Cambridge Isotope Laboratories. Fast performance liquid chromatography (FPLC) protein purification (4 °C) was carried out using an Äkta Purifier from GE Healthcare; all chromatographic columns and the LMW and HMW Gel Filtration Calibration Kit were also from GE Healthcare. Bovine serum albumin and Bradford reagent were from Bio-Rad Laboratories. All steady-state activity assays were performed in an UV-2550 UV/Visible spectrophotometer (Shimadzu). Dithiothreitol (DTT) was from Acros Organics. *Pfu* DNA polymerase was from Stratagene. Restriction enzymes and T4 DNA ligase and pCR-Blunt cloning vector were from Invitrogen and pET-23a(+) expression vector and *E. coli* BL21(DE3) were from Novagen. The mass spectrometer LTQ-XL and LTQ Orbitrap Discovery were from Thermo and the nanoLC Ultra 1D plus was from Eksigent. An iTC_{200} Microcalorimeter was from MicroCal Inc (Northampton, MA). Pre-steady-state measurements were carried out using an Applied Photophysics SX.18MV-R stopped-flow spectrofluorimeter on absorbance mode.

E. coli GMP reductase comparative homology modeling

A *E. coli* three-dimensional model was built by comparative homology modeling using the human type 2 GMP reductase structure as template (PDB ID: 2A7R; hGMPR2),[16] solved by X-ray crystallography at 3.0 Å in complex with GMP. The template structure was used for *E. coli* GMP reductase modeling, as well as to evaluate GMP binding mode to the bacterial enzyme active site. Template selection was based on high primary sequence conservation (68.5% identity and 16.47% strong similarity), and the presence of enzyme substrate bound to its active site. Target and template pair-wise sequence alignment required a single gap inclusion in human GMP reductase primary sequences. The *E. coli* GMP reductase model was built by restrained-based homology modeling implemented in MODELLER9v1,[47] with the standard protocol of the comparative protein structure modeling methodology, by satisfaction of spatial restrains.[48,49] Atomic coordinates of GMP heteroatoms were copied from the template structure into the *E. coli* GMP reductase model. The best model was selected according to MODELLER objective function[50] and subjected to energy minimization for amino acid side chain and main chain rearrangements with the GROMACS package[51] using the 43a1 force-field. The system was submitted to an initial steepest descent energy minimization in vacuum with a maximum number of 400 minimization steps, followed by a maximum of 3000 steps of conjugate gradient energy minimization. The program PROCHECK[52] was employed to analyze the stereochemical quality of the model, as previously described.[53] Structural correspondence between the *E. coli* model and human GMP reductase template was evaluated by their root-mean square deviation (RMSD). H-bond interactions were evaluated with LIGPLOT v4.4.2,[54] considering an atomic distance cut off of 3.9 Å (program default values). Images were generated with PyMOL Molecular Graphic System V1.3 (Schrödinger, LLC).

Amplification and cloning of the *E. coli guaC* gene

The oligonucleotide primer sequences of the *E. coli guaC* structural gene were 5′-AA*CATATG*CGTATTGAAGAAGATCTGAAGTTAGGTTTTAAAGACG-3′ (forward) and 3′-AA*GGATCC*TCATTACAGGTTGTTGAAGATGCGGTTTTCTTGTTCC-5′ (reverse). The primers were designed to contain, respectively, *Nde*I and *Bam*HI restriction sites (in italics). The DNA fragment (1038 bp) was amplified using *Pfu* DNA polymerase, ligated into the pCR-Blunt cloning vector, and transformed into *E. coli* DH10B cells. Plasmid DNA recovered from these cells was digested with the

View Online

Downloaded by Pontificia Universidade Catolica do Rio Grande do Sul on 28 February 2011
Published on 07 February 2011 on http://pubs.rsc.org | doi:10.1039/C0MB00245C

restriction enzymes *Nde*I and *Bam*HI, and the isolated insert was ligated into the pET-23a(+) expression vector, previously treated with the same restriction enzymes. The sequence of the *E. coli guaC* gene was determined by automated DNA sequencing to confirm the identity, integrity, and absence of PCR-introduced mutations in the cloned fragment.

Expression of recombinant GMP reductase

The recombinant plasmid pET-23a(+)::*guaC* was transformed into *E. coli* BL21(DE3) cells, and these were selected on Luria-Bertani (LB) agar plates containing 50 μg mL^{-1} ampicillin. LB medium (60 mL) containing 50 μg mL^{-1} ampicillin was inoculated with a single colony and cells were grown overnight. The culture (10 mL) was inoculated in LB medium (500 mL) with the same antibiotic concentration, and, as soon as $OD_{600\ nm}$ reached a value of 0.6, culture was grown for additional 24 h at 180 rpm and 37 °C without IPTG induction. Cells (15 g) were harvested by centrifugation at 7690*g* for 30 min at 4 °C and were stored at –20 °C. Soluble and insoluble fractions were analyzed by 12% SDS-PAGE and Coomassie staining.

Purification of recombinant GMP reductase

Approximately 2.8 g of frozen cells were resuspended in 14 mL of 100 mM tris(hydroxymethyl)aminomethane (Tris; buffer A), pH 7.8, and incubated with lysozyme (0.2 mg mL^{-1}) for 30 min with stirring. Cells were disrupted by sonication, and centrifuged at 38 900*g* for 30 min to remove cells debris. Streptomycin sulfate was added to the supernatant up to 1% (wt/vol), stirred for 30 min to precipitate nucleic acids, and centrifuged at 38 900*g* for 30 min. The resulting supernatant was dialyzed against buffer A (2 × 2 L; 2 h each) using a dialysis tubing with a molecular weight exclusion limit of 12–14 kDa. The sample was clarified by centrifugation at 38 900*g* for 30 min and loaded on a FPLC 2.6 cm × 8.2 cm Q-Sepharose Fast Flow anion exchange column, pre-equilibrated with buffer A, washed with 5 column volumes of buffer A, and the adsorbed material was eluted with a linear gradient (0-40%) of 20 column volumes of 100 mM Tris pH 7.8 containing 500 mM NaCl (buffer B) at 1 mL min^{-1}. The adsorbed recombinant GMP reductase was eluted at approximately 145 mM NaCl concentration, with substantial removal of contaminants. All fractions were analyzed by SDS-PAGE electrophoresis, and the ones containing the target protein were pooled and concentrated to 8.5 mL using an Amicon ultrafiltration cell (molecular weight cutoff 30 kDa). The soluble sample was loaded on a 2.6 cm × 60 cm HiPrep Sephacryl S-200 High Resolution size exclusion column, which was previously equilibrated with buffer A, and isocratically eluted with buffer A at a flow rate of 0.25 mL min^{-1}. This step was employed to further purify the recombinant protein and to remove salt from the sample, thereby allowing protein preparation for the next chromatographic step. Fractions containing the target protein were pooled and the soluble sample was loaded on a 1.6 cm × 10 cm Mono Q High Resolution anion exchange column, pre-equilibrated with buffer A. The column was washed with 5 column volumes, and the adsorbed proteins were eluted with a linear gradient (0–40%) of 20 column volumes of buffer B, and the target protein eluted at approximately 155 mM NaCl concentration. The active fractions containing the target protein were pooled and dialyzed against buffer A (2 × 2 L; 2 h each) in order to remove the remaining salt. Protein concentration was determined by Bradford's method using bovine serum albumin as standard.[55]

Quaternary structure analysis of *E. coli* GMP reductase

The homogeneous sample was submitted to ESI-MS in order to confirm the identity of *E. coli* GMP reductase. The protein was also digested with trypsin and the resulting peptides were separated and analyzed by liquid chromatography associated with mass spectrometry with fragmentation collision induced, and the results were used to identify the amino acid sequence through a search software (Protein Discoverer, Thermo).

The molecular mass of recombinant GMP reductase was determined by gel filtration chromatography using a 1.0 cm × 30 cm High Resolution Superdex 200 column pre-equilibrated with 50 mM Tris, pH 7.5, containing 200 mM NaCl at a flow rate of 0.4 mL min^{-1}. The LMW and HMW Gel Filtration Calibration Kit were used as the protein molecular mass standards in the calibration curve, measuring the elution volumes of several standards (ferritin, catalase, aldolase, ovalbumin, coalbumin, ribonuclease A, and blue dextran 2000), calculating their partition coefficients (K_{av}), and plotting these values against the logarithm of their molecular mass. The K_{av} values were determined as $K_{av} = (V_e - V_o)/(V_t - V_o)$, where V_e is the sample elution volume, V_t is the total bed volume of the column, and V_o is the column void volume, which had been determined by loading blue dextran 2000 into the column. Protein elution was monitored at 215, 254, and 280 nm.

Synthesis of [4*S*-^{2}H]-NADPH

[4*S*-^{2}H]-NADPH was synthesized according to the method of Ottolina and co-workers[56] and purified on a 1.0 cm × 10 cm Mono Q High Resolution anion exchange column. The column was washed with 1 column volume of 100 mM *N*-2-hydroxyethylpiperazine-*N*′-2-ethanesulfonic acid (Hepes), pH 7.0, and the material was eluted with a linear gradient (0–100%) of 5 column volumes of 100 mM Hepes containing 1.0 M NaCl, pH 7.0, at a flow rate of 0.5 mL min^{-1}. The fractions with $A_{260\ nm}/A_{340\ nm} \leq 2.3$ were pooled.

Enzyme activity assay of *E. coli* GMP reductase

The recombinant GMP reductase activity was determined by a continuous spectrophotometric assay monitoring the conversion of NADPH to $NADP^+$ at 340 nm. The standard assay was performed at 25 °C in 100 mM Tris, pH 7.8, with 10 mM DTT, unless stated otherwise.

Determination of apparent steady-state kinetic constants and initial velocity pattern

In order to determine the apparent steady-state kinetic constants, GMP reductase activity was measured (in duplicates) in the presence of varying concentrations of GMP (5–80 μM) and fixed NADPH concentration (100 μM), and varying concentrations of NADPH (5–120 μM) and fixed GMP concentration (100 μM), in 100 mM Tris, pH 7.8, buffer

 This journal is © The Royal Society of Chemistry 2011

View Online

Downloaded by Pontificia Universidade Catolica do Rio Grande do Sul on 28 February 2011
Published on 07 February 2011 on http://pubs.rsc.org | doi:10.1039/C0MB00245C

containing 10 mM DTT in a total volume of 500 μL. The enzyme specificity for NADPH was evaluated measuring the enzymatic activity in the presence of varying concentrations of NADH (20–200 μM) at a fixed-saturating concentration of GMP (100 μM). To determine the true steady-state kinetic parameters and initial velocity patterns, enzymatic activity was measured in the presence of varying concentrations of GMP (1–60 μM) and several fixed-varied NADPH concentrations (1–60 μM). Enzyme activity was determined in an UV-2550 UV/Visible spectrophotometer (Shimadzu) by monitoring the decrease in absorbance at 340 nm (ε_{340nm} = 6220 M^{-1} cm^{-1}) upon GMP reductase-catalyzed conversion of NADPH to $NADP^+$. One unit of enzyme activity was defined as the amount of protein that catalyzes the consumption of 1 μmol of NADPH per minute at 25 °C.

Isothermal titration calorimetry

ITC experiments were carried out using the iTC_{200} Microcalorimeter. The reference cell (200 μL) was loaded with water during all experiments and the sample cell (200 μL) was filled with *E. coli* GMP reductase at a concentration of 122 μM in buffer A. The injection syringe (39.7 μL) was filled with substrates or products at different concentrations, GMP at 0.75 mM, NADPH at 3.5 mM, $NADP^+$ at 1.0 mM, and IMP at 1.0 mM, and the ligand binding isotherms were measured by direct titration (ligand into macromolecule). The same buffer was used to prepare all ligand solutions. The stirring speed was 500 rpm at 25 °C with constant pressure for all ITC experiments. Titration first injection (0.5 μL) was not used in data analysis and was followed by 17 injections of 2.2 μL each at 180 s intervals. Control titrations (ligand into buffer) were performed in order to subtract the heats of dilution and mixing for each experiment prior to data analysis. All data were evaluated utilizing the Origin 7 SR4 software (Microcal, Inc.).

pH-rate profiles

The dependence of kinetic parameters on pH was determined by measuring initial velocities in the presence of varying concentrations of one substrate and saturating levels of the other, in a buffer mixture of 500 mM 2-(*N*-morpholino)-ethanesulfonic acid (MES)/Hepes/2-(*N*-cyclohexylamino)-ethanesulfonic acid (CHES) over the following pH values: 6.0 (10–160 μM varying GMP concentration and fixed concentration of NADPH at 240 μM, and 10–160 μM varying NADPH concentration and fixed concentration of GMP at 240 μM), 6.5 (2–60 μM varying GMP concentration and fixed concentration of NADPH at 100 μM, and 2–60 μM varying NADPH concentration and fixed concentration of GMP at 100 μM), 7.0 (2–60 μM varying GMP concentration and fixed concentration of NADPH at 100 μM, and 2–60 μM varying NADPH concentration and fixed concentration of GMP at 100 μM), 7.5 (5–80 μM varying GMP concentration and fixed concentration of NADPH at 100 μM, and 5–80 μM varying NADPH concentration and fixed concentration of GMP at 100 μM), 8.0 (5–80 μM varying GMP concentration and fixed NADPH concentration at 100 μM, and 5–80 μM varying NADPH concentration and fixed concentration of GMP at 100 μM), 8.5 (5–60 μM varying GMP concentration and fixed concentration of NADPH at 100 μM, and 5–60 μM varying NADPH concentration and fixed concentration of GMP at 100 μM), 9.0 (5–60 μM varying GMP concentration and fixed concentration of NADPH at 100 μM, and 5–60 μM varying NADPH concentration and fixed concentration of GMP at 100 μM), and 9.5 (2–60 μM varying GMP concentration and fixed concentration of NADPH at 100 μM, and 2–60 μM varying NADPH concentration and fixed concentration of GMP at 100 μM). Prior to performing the pH-rate profiles, the recombinant enzyme was incubated over a broader pH range and assayed under standard conditions to identify denaturing pH values and to ensure enzyme stability at the tested pH range.

Energy of activation

In order to determine the energy of activation of the GMP reductase-catalyzed reaction, initial velocities were measured in the presence of varying concentrations of one (GMP 1–60 μM) (NADPH 1–80 μM) substrate and saturating levels of the other (100 μM), at temperatures ranging from 15 to 35 °C. GMP reductase was incubated for several minutes in all temperatures tested and assayed under standard conditions to ensure enzyme stability under all temperatures.

Deuterium kinetic isotope effects and proton inventory

Primary deuterium kinetic isotope effects were determined by measuring initial rates using a saturating level of GMP (100 μM) and varying concentrations of either NADPH (4–60 μM) or [4*S*-^{2}H]-NADPH (1–60 μM).

Solvent kinetic isotope effects were determined by measuring initial velocities using a saturating level of one substrate (100 μM) and varying concentrations of the other (GMP: 4–60 μM; NADPH: 4–60 μM) in either H_2O or 90 atom% D_2O. The proton inventory was determined using saturating concentrations of both substrates (100 μM) at various mole fractions of D_2O.

Multiple kinetic isotope effects were measured by determining the solvent isotope effects using [4*S*-^{2}H]-NADPH (NADPD) as the varied substrate.

An equilibrium isotope effect ($^DK_{eq}$) was determined by measuring the equilibrium constant in the presence of either NADPH or [4*S*-^{2}H]-NADPH. These equilibrium constants were measured as described by Leu and Cook.[57] In short, the ratio of [NADPH]/[$NADP^+$] was fixed at 1 and the ratio of [IMP]/[GMP] were varied from 0.1 to 30 at fixed concentration of NH_4Cl. A plot of the change in NADPH concentration *versus* [IMP]/[GMP] ratio crosses the abscissa at a value equal to K_{eq}.[57]

The notation utilized to express isotope effects is that of Northrop[30] as extended by Cook and Cleland.[58]

Pre-steady-state kinetics

Pre-steady-state kinetic measurements of the reaction catalyzed by *E. coli* GMP reductase were performed to determine whether product release is part of the rate-limiting step. The decrease in absorbance was monitored at 340 nm (1 mm split width = 4.65 nm spectral band), at 25 °C, using a split time base (2–50 s; 400 data points for each time base). The experimental conditions were 10 μM *E. coli* GMP reductase,

View Online

Downloaded by Pontificia Universidade Catolica do Rio Grande do Sul on 28 February 2011
Published on 07 February 2011 on http://pubs.rsc.org | doi:10.1039/C0MB00245C

10 mM DTT, 250 μM GMP and 250 μM NADPH in 100 mM Tris-HCl, pH 7.8 (mixing chamber concentrations). The experimental conditions for the control experiment were 10 μM *E. coli* GMP reductase, 10 mM DTT, and 250 μM NADPH in 100 mM Tris-HCl, pH 7.8 (mixing chamber concentrations). The dead time of the stopped-flow equipment is 1.37 ms.

Data analysis

Values of the kinetic parameters and their respective errors were obtained by fitting the data to the appropriate equations by using the nonlinear regression function of SigmaPlot 9.0 (SPSS, Inc.). Initial rate data at single concentration of the fixed substrate and varying concentrations of the other were fitted to eqn (1).[17]

$$v = \frac{VA}{K + A} \tag{1}$$

The family of lines intersecting to the left of the *y*-axis in double-reciprocal plots was fitted to eqn (2), which describes a mechanism involving ternary complex formation and a sequential substrate binding.[59]

$$v = \frac{VAB}{K_{ia}K_b + K_aB + K_bA + AB} \tag{2}$$

For eqn (1) and (2), v is the initial velocity, V is the maximal initial velocity, A and B are the concentrations of the substrates (GMP and NADPH), K_a and K_b are their respective Michaelis constants, and K_{ia} is the dissociation constant for enzyme–substrate A binary complex formation.

pH-rate profiles data were fitted to eqn (3), (4) or (5), where y is the kinetic parameter, C is the pH-independent value of y, H is the proton concentration, and K_a and K_b are, respectively, the apparent acid and base dissociation constants for ionizing groups, and K_0 is the product of two apparent dissociation constants.[60]

$$\log y = \log\left(\frac{C}{1 + \frac{H}{K_a} + \frac{K_b}{H}}\right) \tag{3}$$

$$\log y = \log\left(\frac{C}{1 + \frac{H}{K_a} + \frac{H^2}{K_0} + \frac{K_b}{H} + \frac{K_0}{H^2}}\right) \tag{4}$$

$$\log y = \log\left(\frac{C}{1 + \left(\frac{H}{K_{a1}}\right)\left(1 + \frac{H}{K_{a2}}\right)}\right) \tag{5}$$

Eqn (3) describes a bell-shaped pH profile for a group that must be protonated for binding/catalysis and another group that must be unprotonated for binding/catalysis, and participation of a single ionizing group for the acidic limb (slope value of +1) and participation of a single ionizing group for the basic limb (slope value of −1). Eqn (4) describes a bell-shaped pH-rate profile that starts with a slope of +2 in the acidic limb and goes to an eventual slope of −2 in the basic limb, suggesting participation of two ionizing groups in each limb. Eqn (5) describes a pH-rate profile for two groups that need to be unprotonated for binding (slope of +2 for the acidic limb). Unless the p*K*s of the groups are at least 3 pH units apart, there will not be a linear region with a slope of +1.

The data for temperature effects were fitted to eqn (6), where k is the maximal reaction rate, E_a is the energy of activation, T is the temperature in Kelvin, R is the gas constant (1.987 cal K^{-1} mol^{-1}), and A is a pre-exponential factor that correlates collision frequency and the probability of the reaction occurring when reactant molecules collide.

$$\log k = -\left(\frac{E_a}{2.3R}\right)\left(\frac{1}{T}\right) + \log A \tag{6}$$

Kinetic isotope effects data were fitted to eqn (7), which assumes isotope effects on both V/K and V. In this equation, $E_{V/K}$ and E_V are the isotope effects minus 1 on V/K and V, respectively, and F_i is the fraction of isotopic label in substrate A.[36]

$$v = \frac{VA}{K(1 + F_iE_{V/K}) + A(1 + F_iE_V)} \tag{7}$$

ITC data were fitted to eqn (8), where ΔH is the enthalpy of process given by the ITC experiment, ΔG is the Gibbs free energy changes, ΔS is the entropy changes, T is the temperature of the experiment in Kelvin, R is the gas constant (1.987 cal K^{-1} mol^{-1}), and K_{eq} is the equilibrium binding constant. The dissociation constant, K_d, is the inverse of the equilibrium binding constant, K_{eq}, described in eqn (9).

$$\Delta G = \Delta H - T\Delta S = -RT\ln K_{eq} \tag{8}$$

$$K_d = \frac{1}{K_{eq}} \tag{9}$$

The pre-steady-state time course of the reaction was fitted to eqn (10) for a single exponential decay, in which A is the absorbance at time t, A_0 is the absorbance at time zero, and k is the apparent first-order rate constant for product formation.[39]

$$A = A_0e^{-kt} \tag{10}$$

Acknowledgements

This work was supported by funds of Millennium Initiative Program (CNPq) and National Institute of Science and Technology on Tuberculosis (INCT-TB), MCT-CNPq, Ministry of Health—Department of Science and Technology (DECIT)—Secretary of Health Policy (Brazil) to D.S.S. and L.A.B. D.S.S. (CNPq, 304051/1975-06) and L.A.B. (CNPq, 520182/99-5) are Research Career Awardees of the National Research Council of Brazil (CNPq). R.G.D. is a postdoctoral fellow of CNPq. L.A.R. acknowledges an MSc scholarship awarded by CAPES, A.B. acknowledges her PhD scholarship awarded by BNDES, and L.K.B.M. a PhD scholarship awarded by CNPq.

 This journal is © The Royal Society of Chemistry 2011

View Online

Downloaded by Pontificia Universidade Catolica do Rio Grande do Sul on 28 February 2011
Published on 07 February 2011 on http://pubs.rsc.org | doi:10.1039/C0MB00245C

References

1 H. J. J. Nijkamp and P. G. DeHaan, *Biochim. Biophys. Acta*, 1967, **147**, 31–40.
2 Y. Deng, Z. Wang, K. Ying, S. Gu, C. Ji, Y. Huang, X. Gu, Y. Wang, Y. Xu, Y. Li, Y. Xie and Y. Mao, *Int. J. Biochem. Cell Biol.*, 2002, **34**, 1035–1050.
3 S. C. Andrews and J. R. Guest, *Biochem. J.*, 1988, **255**, 35–43.
4 R. E. Roberts, C. I. Lienhard, C. G. Gaines, J. M. Smith and J. R. Guest, *J. Bacteriol.*, 1988, **170**, 463–467.
5 C. E. Benson, B. A. Brehmeyer and J. S. Gots, *Biochem. Biophys. Res. Commun.*, 1971, **403**, 1089–1094.
6 B. B. Garber, B. U. Jochimsen and J. S. Gots, *J. Bacteriol.*, 1980, **143**, 105–111.
7 A. I. Kessler and J. S. Gots, *J. Bacteriol.*, 1985, **164**, 1288–1293.
8 M. F. Renart and A. Silero, *Biochim. Biophys. Acta*, 1976, **341**, 178–186.
9 T. Spector and T. E. Jones, *Biochem. Pharmacol.*, 1982, **31**, 3891–3897.
10 J. J. Mackenzie and L. B. Sorensen, *Biochim. Biophys. Acta*, 1973, **327**, 282–294.
11 T. Spector, T. E. Jones and R. L. Miller, *J. Biol. Chem.*, 1979, **254**, 2308–2315.
12 S. Henikoff and J. M. Smith, *Cell (Cambridge, Mass.)*, 1989, **58**, 1021–1022.
13 J. Zhang, W. Zhang, D. Zou, G. Chen, T. Wan, M. Zhang and X. Cao, *J. Cancer Res. Clin. Oncol.*, 2003, **129**, 76–83.
14 D. Salvatore, T. Bartha and P. R. Larsen, *J. Biol. Chem.*, 1998, **273**, 31092–31096.
15 T. Page, S. J. Jacobsen, R. M. Smejkal, J. Scheele, W. L. Nyhan, J. H. Magnun and R. K. Robbins, *Cancer Chemother. Pharmacol.*, 1985, **15**, 59–62.
16 J. Li, Z. Wei, M. Zheng, X. Gu, Y. Deng, R. Qiu, F. Chen, C. Ji, W. Gong, Y. Xie and Y. Mao, *J. Mol. Biol.*, 2006, **355**, 980–988.
17 V. Henri, L. Michaelis and M. L. Menten, *Biochem. Z.*, 1913, **49**, 333–369.
18 J. D. Thompson, D. G. Higgins and T. J. Gibson, *Nucleic Acids Res.*, 1994, **22**, 4673–4680.
19 K. C. Kelley, K. J. Huestis, D. A. Austen, C. T. Sanderson, M. A. Donohue, S. K. Stickel, E. S. Kawasaki and M. S. Osburne, *Gene*, 1995, **156**, 33–36.
20 C. Rizzi, J. Frazzon, F. Ely, P. G. Weber, I. O. Fonseca, M. Gallas, J. S. Oliveira, M. A. Mendes, B. M. Souza, M. S. Palma, D. S. Santos and L. A. Basso, *Protein Expression Purif.*, 2005, **40**, 23–30.
21 G. Biazus, C. Z. Schneider, M. S. Palma, L. A. Basso and D. S. Santos, *Protein Expression Purif.*, 2009, **66**, 185–190.
22 Z. A. Sanchez-Quitian, C. Z. Schneider, R. G. Ducati, W. F. de Azevedo, Jr., C. Bloch, Jr., L. A. Basso and D. S. Santos, *J. Struct. Biol.*, 2010, **169**, 413–423.
23 T. H. Grossman, E. S. Kawasaki, S. R. Punreddy and M. S. Osburne, *Gene*, 1998, **209**, 95–103.
24 F. W. Studier, *Protein Expression Purif.*, 2005, **41**, 207–234.
25 A. Levitzki and D. E. Koshland, Jr, *Proc. Natl. Acad. Sci. U. S. A.*, 1969, **62**, 1121–1128.
26 A. Velazquez-Campoy and E. Freire, *Biophys. Chem.*, 2005, **115**, 115–124.
27 J. E. Ladbury and M. L. Doyle, *Biocalorimetry II*, Wiley, London, 2004, 1st edn, p. 259.
28 P. Kwong, M. L. Doyle, D. J. Casper, C. Cicala, S. A. Leavitt, S. Majeed, T. D. Steenbeke, M. Venturi, I. Chaiken, M. Fung, H. Katinger, P. W. Parren, J. Robinson, D. Van Ryk, L. Wang, D. R. Burton, E. Freire, R. Wyatt, J. Sodroski, W. A. Hendrickson and J. Arthos, *Nature*, 2002, **420**, 678–682.
29 G. Bulaj, T. Kortemme and D. P. Goldenberg, *Biochemistry*, 1998, **37**, 8965–8972.
30 D. B. Northrop, *Biochemistry*, 1975, **14**, 2644–2651.
31 J. H. Richards, *Enzymes*, Academic Press, New York, 1970, 2nd edn, p. 321.
32 P. F. Cook, *Enzyme Mechanism from Isotope Effects*, CRC Press, Boca Raton, 1991, pp. 203–228.
33 P. F. Cook, *Isot. Environ. Health Stud.*, 1998, **34**, 3–17.
34 M. P. Patel, W. Liu, J. West, D. Tew, T. D. Meek and S. H. Thrall, *Biochemistry*, 2005, **44**, 16753–16765; R. G. Silva, L. P. S. de Carvalho, J. S. Blanchard, D. S. Santos and L. A. Basso, *Biochemistry*, 2006, **45**, 13064–13073.
35 D. B. Northrop, *Methods*, 2001, **24**, 117–124.
36 P. F. Cook and W. W. Cleland, *Enzyme Kinetics and Mechanism*, Garland Science Publishing, New York, 2007, ch. 9, pp. 253–323.
37 P. F. Cook, J. S. Blanchard and W. W. Cleland, *Biochemistry*, 1980, **19**, 4853–4858.
38 J. G. Belasco, W. J. Albery and J. R. Knowles, *J. Am. Chem. Soc.*, 1983, **105**, 2475–2477.
39 K. Hiromi, *Kinetics of Fast Enzyme Reactions: Theory and Practice*, Kodansha Ltd., Tokyo, 1979, ch. 4, pp. 188–253.
40 J. G. Robertson, *Biochemistry*, 2005, **44**, 5561–5571; J. G. Robertson, *Curr. Opin. Struct. Biol.*, 2007, **17**, 674–679.
41 M. L. Bianconi, *Biophys. Chem.*, 2007, **126**, 59–64.
42 J. E. Ladbury, G. K. Klebe and E. Freire, *Nat. Rev. Drug Discovery*, 2010, **9**, 23–27.
43 D. E. Almonacid, E. R. Yera, J. B. O. Mitchell and P. C. Babbitt, *PLoS Comput. Biol.*, 2010, **6**(3), e1000700.
44 C. Lugnier, *Pharmacol. Ther.*, 2006, **109**, 366–398.
45 H. T. Zhang, *Curr. Pharm. Des.*, 2009, **15**, 1688–1698.
46 A. C. Bishop and V. L. Chen, *J. Chem. Biol.*, 2010, **2**, 1–9.
47 A. Sali and T. L. Blundell, *J. Mol. Biol.*, 1993, **234**, 779–815.
48 M. A. Martí-Renom, A. C. Stuart, A. Fiser, R. Sánchez, F. Melo and A. Sali, *Annu. Rev. Biophys. Biomol. Struct.*, 2000, **29**, 291–325.
49 A. Sali and J. P. Overington, *Protein Sci.*, 1994, **3**, 1582–1596.
50 M. Y. Shen and A. Sali, *Protein Sci.*, 2006, **15**, 2507–2524.
51 D. van der Spoel, E. Lindahl, B. Hess, G. Groenhof, A. E. Mark and H. J. C. Berendsen, *J. Comput. Chem.*, 2005, **26**, 1701–1718.
52 R. A. Laskowski, M. W. MacArthur, D. S. Moss and J. M. Thornton, *J. Appl. Crystallogr.*, 1993, **26**, 283–291.
53 I. O. Fonseca, R. G. Silva, C. L. Fernandes, O. N. de Souza, L. A. Basso and D. S. Santos, *Arch. Biochem. Biophys.*, 2007, **457**, 123–133.
54 A. C. Wallace, R. A. Laskowski and J. M. Thornton, *Protein Eng., Des. Sel.*, 1995, **8**, 127–134.
55 M. M. Bradford, R. A. Mcroire and W. L. Williams, *Anal. Biochem.*, 1976, **72**, 248–254.
56 G. Ottolina, S. Riva, G. Carrea, B. Danieli and A. F. Buckman, *Biochim. Biophys. Acta*, 1989, **998**, 173–178.
57 L. S. Leu and P. F. Cook, *Biochemistry*, 1994, **33**, 2667–2671.
58 P. F. Cook and W. W. Cleland, *Biochemistry*, 1981, **20**, 1790–1796.
59 I. H. Segel, *Enzyme kinetics, behavior and analysis of rapid equilibrium and steady-state enzyme systems*, John Wiley & Sons, Inc., New York, 1975, p. 957.
60 P. F. Cook and W. W. Cleland, *Enzyme Kinetics and Mechanism*, Garland Science Publishing, New York, 2007, ch. 10, pp. 325–366.

CAPÍTULO 4

Considerações finais

Considerações finais

O desenho racional de inibidores baseia-se nas informações mecanísticas e estruturais de enzimas-alvo. Esses inibidores compreendem uma parcela de 25% do mercado de medicamentos dos Estados Unidos (Robertson, 2005; Robertson, 2007). Desse modo, a análise mecanística do alvo deve ser sempre uma prioridade nos programas de descoberta de novas drogas que busca o desenho racional de potentes inibidores enzimáticos. Além do mais, a titulação de calorimetria isotérmica tem sido usada como uma importante técnica para determinação direta de parâmetros termodinâmicos e cinéticos de reações enzimáticas (Bianconi, 2007). O reconhecimento das limitações da abordagem de *high-throughput screening* na descoberta de novas drogas fez com que o desenho racional de drogas tivesse uma importância maior (Ladbury, Klebe, Freire, 2010).

O entendimento do modo de ação da enzima GMP redutase de *E. coli* pode fornecer as informações necessárias para desenhar novos inibidores para esta enzima, visto que apesar de presente na flora intestinal de indivíduos sadios, algumas cepas de *E. coli* podem causar infecções intestinais ou extra intestinais em indivíduos sadios, bem como, em pacientes imunocomprometidos (Nataro, Bopp, Fields, Kaper, Strockbine, 2007). Infecções do trato urinário, bacteremia, meningite e diarreia são os sintomas clínicos mais comuns, causados primariamente por um número limitado de clones patogênicos de *E. coli* (Kaper, Nataro, Mobley, 2004). A subespécie enteropatogênica de *E. coli* é

uma importante bactéria causadora de diarreia em países em desenvolvimento, além de ter causado surtos altamente letais em enfermarias neonatais na década de 70 nos EUA (Miqdady, Jiang, Nataro, Dupont, 2002), fatos esses que justificam a busca de inibidores da enzima GMP redutase de *E. coli*.

As enzimas GMP redutase dos gêneros *Salmonella* e *Shigella*, ambos os organismos Gram-negativos patogênicos, podem ser vistas como alvo para o futuro desenvolvimento de inibidores, utilizando como modelo os resultados obtidos para a enzima homóloga de *E. coli*, aqui apresentados, devido à alta identidade entre as enzimas GMP reductase (99,7% com a enzima de *Shigella*) (identidade de 95,1% com a enzima de *Salmonella*). O gênero *Shigella* causa diarreia hemorrágica (disenteria) e diarreia não-hemorrágica (Nataro, Bopp, Fields, Kaper, Strockbine, 2007); o gênero *Salmonella* é classificado em tifoidal e não-tifoidal, sendo que as cepas não-tifoidais geralmente causam infecções intestinais (diarreia, febre e cólicas) e persistem por uma semana ou mais. As cepas tifoidais, por outro lado, causam febre tifoide, uma infecção sanguínea grave, comum em países em desenvolvimento (Nataro, Bopp, Fields, Kaper, Strockbine, 2007).

O desenvolvimento de um inibidor capaz de agir em *Klebsiella pneumoniae*, bactéria causadora de pneumonia, torna-se crítico com o surgimento de cepas resistentes aos carbapenêmicos imipenem e meropenem, um grupo de antibióticos β-lactâmicos de alto espectro de ação, e um dos agentes mais apropriados para o tratamento de infecções causadas por bactérias Gram-negativas multirresistente (Woodford, Tierno, Young, Tysall,

Palepou, Ward, *et al*, 2004). Uma enzima que participa da via de salvamento de purinas e responsável pelos níveis celulares de nucleotídeos púricos, como a GMP redutase, pode ser um alvo molecular específico interessante para o desenvolvimento de drogas que permitam o controle e profilaxia da infecção por *Klebsiella pneumoniae carbapenemase,* além de infecções por *K. pneumoniae* resistentes aos medicamentos de primeira escolha, como por exemplo, penicilinas, cefalosporinas e quinolonas.

Além disso, o entendimento do modo de ação de uma enzima pode ser utilizado para informar anotação funcional de sequências e estruturas recém-determinadas, para selecionar modelos enzimáticos apropriados para estabelecer novas funções, e para refinar as definições nas atuais classificações de EC (Almonacid, Yera, Mitchell, Babbitt, 2010). Os resultados aqui apresentados também podem ajudar o desenho de compostos baseados em função que inibam ou ativem a enzima GMP redutase para conduzir experimentos que revelem o papel biológico da GMP redutase no contexto celular de *E. coli* (Bishop, Chen, 2010).

REFERÊNCIAS BIBLIOGRÁFICAS

Almonacid D E, Yera E R, Mitchell J B O, Babbitt P C, Quantitative comparison of catalytic mechanisms and overall reactions in convergently evolved enzymes: implications for classification of enzyme function, **PLoS Comput. Biol.**, 2010; 6(3): e10000700.

Alberts B, Johnson A, Lewis J, Raff M, Roberts K, Walter P, **Biologia Molecular da Célula**, 5ª ed., Porto Alegre, Editora Artmed, 2010, 1396p.

Andrews S C, Guest J R, Nucleotide sequence of the gene encoding the GMP reductase of *Escherichia coli* K12, **Biochem. J**., 1988; 255:35-43.

Bianconi M L, Calorimetry of enzyme-catalyzed reactions **Biophys. Chem**., 2007; 126(1-3): 59-64.

Bishop A C, Chen V L, Brought to life: targeted activation of enzyme function with small molecules. **J. Chem. Biol**., 2010; 2(1): 1-9.

Chang Z Y, Nygaard P, Chinault A C, Kellems R E, Deduced amino acid sequence of *Escherichia coli* adenosine deaminase reveals evolutionarily conserved amino acid residues: implications for catalytic function**, Biochem**. 1991; 30(8):2273-80.

Devlin T M, **Manual de Bioquímica com correlações clínicas,** 3ª ed., Porto Alegre, Editora Blücher, 2007, 1186p.

Ducati R G, Breda A, Basso L A, Santos D S, Purine salvage pathway in Mycobacterium tuberculosis, **Curr. Med. Chem**., aceito em 2010.

el Kouni M H, Potential chemotherapeutic targets in the purine metabolism of parasites, **Pharmaco Ther**., 2003; 99(3):283-309.

Garber B B, Jochimsen B U, Gots J S, Glutamine and related analogs regulate guanosine monophosphate reductase in *Salmonella typhimurium*, **J Bacteriol**., 1980; 143(1):105-11.

Gilbert H J, Lowe C R, Drabble W T, Inosine 5'-monophosphate dehydrogenase of *Escherichia coli*. Purification by affinity chromatographic, subunit structure and inhibition by guanosine 5'-monophosphate, **Biochem. J.**, 1979; 183:481-489

Harlow K W, Nygaard P, Hove-Jensen B Cloning and characterization of the *gsk* gene encoding guanosine kinase of *Escherichia coli* **J. Bacteriol**., 1995; 177(8):2236-40.

He B, Smith J M, Zalkin H, *Escherichia coli* purB gene: cloning, nucleotide sequence, and regulation by purR, **J. Bacteriol**, 1992; 174(1):130-6.

Hershey H V, Taylor M W, Nucleotide sequence and deduced amino acid sequence of *Escherichia coli* adenine phosphoribosyltransferase and comparison with other analogous enzymes, **Gene**, 1983; 43(3):287-293.

Hochstadt J, Hypoxanthine phosphoribosyltransferase and guanine phosphoribosyltransferase from enteric bacteria, **Methods Enzymol**., 1978; 51:558-567.

Houlberg U, Jensen K F, Role of hypoxanthine and guanine in regulation of *Salmonella typhimurium pur* gene expression, **J. Bacteriol.**, 1983; 155:837-845.

Jensen K F, Nygaard P, Purine nucleoside phosphorylase from *Escherichia coli* and *Salmonella typhimurium*. Purification and some properties, **Eur. J. Biochem**., 1975; 51:253-265.

Kaper J B, Nataro J P, Mobley H L, Pathogenic *Escherichia coli*, **Nat. Rev. Microbiol.**, 2004; 2:123-140.

Kessler A I, Gots J S, Regulation of *guaC* expression in *Escherichia coli*, **J. Bacteriol.**, 1985; 164:1288-1293.

Knöfel T, Sträter N, X-ray structure of the *Escherichia coli* periplasmic 5'-nucleotidase containing a dimetal catalytic site, **Nat. Struct. Biol**., 1999; 6(5):448-53.

Ladbury J E, Klebe G K, Freire E, Adding calorimetric data to decision making in lead discovery: a hot tip, **Nat. Rev. Drug Discov**., 2010; 9(1); 23-27.

Li J, Wei Z, Zheng M, Gu X, Deng Y, Qiu R et. al., Crystal structure of human guanosine monophosphate reductase 2 (GMPR2) in complex with GMP, **J Mol. Biol**. 2006; 355:980-988.

Lugnier C, Cyclic nucleotide phosphodiesterase (PDE) superfamily: a new target for the development of specific therapeutic agents., **Pharmacol. Ther.** 2006, 109:366-398;

Mackenzie J J, Sorensen L B, Guanosine 5'-phosphate reductase of human erythrocytes, **Biochim. Biophys. Acta**, 1973; 327(2):282-94.

Mager J, Magasanik B, Guanosine 5'-phosphate reductase and its role in the interconversion of purine nucleotides, **J. Biol Chem**, 1960; 235:1474-78.

Miqdady M S, Jiang Z D, Nataro J P, Dupont H L, Detection of enteroaggregative Escherichia coli with formalin-preserved HEp-2 cells. **J. Clin. Microbiol.**, 2002; 40:3066-3067.

Nataro J P, Bopp C A, Fields P I, Kaper J B, Strockbine, Escherichia, Shigella, and Salmonella. In: Murray P R (Ed.). **Manual of Clinical Microbiology**. Washington: ASM PRESS, 2007 p. 670-683.

Neidhardt F, ***Escherichia coli* and *Salmonella*, Cellular and Molecular Biology**. Washington: ASM PRESS, 2005.

Nygaard P, Utilization of preformed purine bases and nucleosides. In: A. Munch-Petersen (ed). **Metabolism of nucleotides, nucleosides, and nucleobases in Microrganism**. Academic Press, Inc., London, 1983, p 27-93.

Renart M F, Sillero A, GMP reductase in *Artemia salina*, **Biochim. Biophys. Acta,** 1974; 341(1):178-86.

Roberts R E, Lienhard C I, Gaines C G, Smith J M, Guest J R, Genetic and molecular characterization of the *guaC-nadC-aroP* region of *Escherichia coli* K12, **J. Bacteriol**. 1988; 170(1):463-7.

Robertson J G, Mechanistic basis of enzyme-targeted drugs, **Biochem.**, 2005; 44(15): 5561-5571.

Robertson J G, Enzymes as a special class of therapeutic target: clinical drugs and modes of action, **Curr. Opin. Struct**. **Biol**., 2007; 17(6): 674-679.

Sakamoto N, Hatfield G W, Moyed H S, Physical properties and subunit structure of xanthosine 5'phosphate aminase, **J. Biol. Chem**., 1972; 247:5880-7.

Smith C, Marks A D, Lieberman M, **Marks' Basic Medical Biochemistry**, a clinical approach, 2ª ed., Estados Unidos, Editora Lippincott Williams & Wilkins., 2005, 977p.

Spector T, Jones T E, Guanosine 5'-monophosphate reductase from *Leishmania donovani*. A possible chemotherapeutic target, **Biochem. Pharmacol**., 1982; 31(23):3891-7.

Spector T, Jones T E, Miller R L, Reaction mechanism and specificity of human GMP reductase. Substrates, inhibitors, activators, and inactivators, **J Biol. Chem**. 1979; 254(7):2308-15.

Stayton M M, Rudolph F B, Fromm H J, Regulation, genetics, and properties of adenylosuccinate synthetase: a review, **Curr. Top. Cell Regul**., 1983; 22:104-41.

Woodford N, Tierno P M Jr, Young K, Tysall L, Palepou M F, Ward E, *et al*. Outbreak of *Klebsiella pneumoniae* producing a new carbapenem-hydrolyzing class A beta-lactamase, KPC-3, in a New York Medical Center, **Antimicrob Agents Chemother**. 2004 Dec; 48(12):4793-9.

Voet D, Voet J G, **Bioquímica**, 3ª ed., Porto Alegre, Editora Artmed, 2006, 1616p.

Zhang H T, Cyclic AMP-specific phosphodiesterase-4 as a target for the development of antidepressant drugs, **Curr. Pharm. Des.** 2009, 15:1688-1698.

Anexo

Clonagem, expressão, purificação e caracterização da polinucleotídeo fosforilase (PNPase) de *Mycobacterium tuberculosis* para validação como alvo para o desenvolvimento racional de amostra atenuada

Introdução

Estudos epidemiológicos estimam que um terço da população mundial esteja infectado pelo *Mycobacterium tuberculosis*, o principal agente etiológico da tuberculose (TB) (Zahrt, 2003). Anualmente, ocorrem cerca de 8 a 10 milhões de novos casos de TB e cerca de 3 milhões de mortes, de forma que o *M. tuberculosis* é responsável pela maior mortalidade causada por um único agente infeccioso (Pasqualoto, 2001). O rápido aumento no número de casos de TB, a emergência de cepas resistentes do bacilo e o efeito devastador da co-infecção por HIV levam à urgente necessidade do desenvolvimento de novas drogas antimicobacterianas.

A enzima Polinucleotídeo Fosforilase (PNPase) de *M. tuberculosis* é codificada pelo gene *gpsI* (Rv2783c) que possui 2.259 nucleotídeos que são traduzidos em 752 aminoácidos formando uma proteína de massa molecular de 80kDa. A PNPase é uma 3´-5´-exorribonuclease que possui um papel chave no metabolismo de RNAs de bactérias (Grunberg-Manago & Ochoa 1955, Godefroy-Colburn & Grunberg-Manago 1972 e Colburn & Mackie 1999). A

enzima PNPase converte nucleotídeos difosfatados em polirribonucleotídeos em condições de baixa concentração de fosfato inorgânico (Sulewiski, 1989 e Littauer & Soreq, 1982). Esta enzima foi a primeira a ser descoberta que catalisa a síntese *de novo* de polirribonucleotídeos com uma ligação 3´,5´-fosfodiéster (Littauer, 2005). Estudos mostram que na reação direta, longo polirribonucleotídeos são sintetizados de maneira progressiva a partir de diversos ribonucleotídeos difosfatados. Cada um dos quatros ribonucleotídeos comuns podem servir separadamente como substrato. Na reação reversa, a PNPase é uma 3´a 5´exorribonuclease que catalisa gradualmente a fosforólise de polirribonucleotídeos de fita simples, liberando ribonucleotídeos difosfatados (Littauer, 2005).

Esta enzima, que possui atividade 3`-5` exonuclease e 5`-3` polimerase, atua de forma fundamental no complexo degradossomo, sendo considerada um regulador global de expressão gênica (Jones et al., 2003), tendo seu papel caracterizado em diversos microorganismos como *E. coli* (Mohanty & Kushner, 2000)*, Bacillus subtillis* (Mitra et. al., 1996), *Salmonella enterica* (Clements et al., 2002) e *Streptomyces antibioticus* (Bradley & Jones, 2003). A demonstração da atuação da PNPase como regulador global na expressão de fatores de virulência em *Salmonella enterica*, onde uma única mutação no gene que codifica para a PNPase afeta o nível de genes de transcritos envolvidos em virulência e reforça o estabelecimento de infecção persistente, traz novas propostas para o estudo desta enzima em *M. tuberculosis*, já que assim como no caso de *S. entérica*, o bacilo é um patógeno intracelular facultativo que causa infecção aguda e

persistente. O papel dessa enzima em *M. tuberculosis*, ainda sem evidências experimentais, faz necessário o estudo e caracterização desta no esforço de elucidar os mecanismos envolvidos na virulência e invasão do bacilo.

Resultados

Inicialmente foi realizada a amplificação da região codificante do gene *gpsI* de *M. tuberculosis* a partir do DNA genômico da cepa de *M. tuberculosis* H37Rv através da técnica de reação em cadeia pela polimerase (PCR) onde foi utilizada a enzima *Pfu DNA polymerase* (Stratagene), a qual possui uma alta fidelidade na polimerização, com atividade 3'-5' exonuclease (Figura A1).

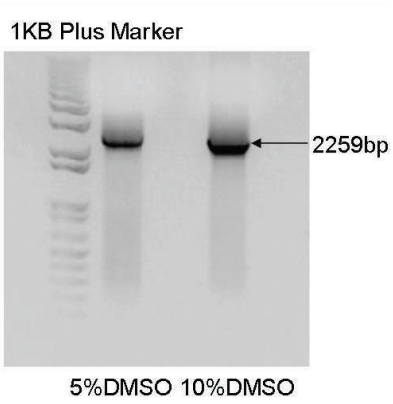

Figura A1: Gel de agarose com 5% de brometo de etídeo, mostrando a amplificação do gene *gpsI* com 5 e 10% de DMSO

O produto da reação de PCR com 10% DMSO foi inserido na região de clonagem do vetor pCR-Blunt® (Invitrogen) para a obtenção dos plasmídeos recombinantes. Após a escolha dos plasmídeos recombinantes contendo os

fragmentos do gene *gpsI*, estes foram clivados com as enzimas de restrições para a liberação dos insertos e posterior ligação com o vetor de expressão pET-23a(+)® (Novagen) pré-clivado com as mesmas enzimas. O DNA plasmidial extraído foi clivado com as endonucleases *Nde*I/*H*indIII para confirmação dos insertos clonados (Figura A2). O sequenciamento dos fragmentos clonados, pelo método automático confirmou a identidade do gene *gpsI* clonado bem como a ausência de mutações.

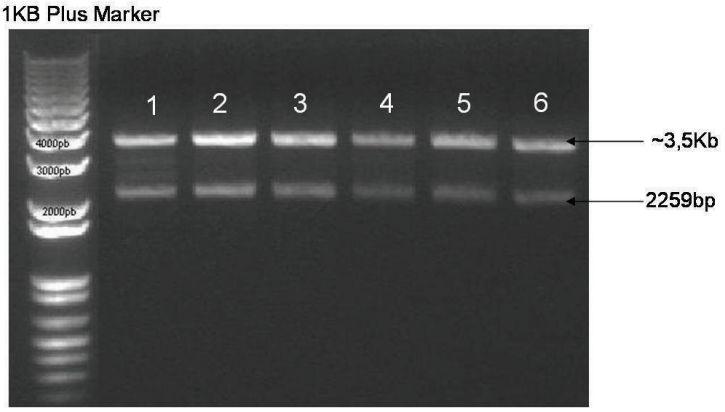

Figura A2: Clivagem do plasmídeo pET 23a(+)::*gpsI* mostrando a liberação de um fragmento de aproximadamente 2000bp correspondente ao gene *gpsI* de *M. tuberculosis*

Após a confirmação dos fragmentos clonados, o plasmídeo recombinante contendo o inserto pET-23a(+)::*gpsI* foi transformado em diferentes cepas de células de *E. coli* para obter a expressão da proteína PNPase sua forma solúvel, onde também foram testados diferentes meios de cultivo, temperatura de crescimento e presença de um indutor IPTG. A análise das frações solúveis e insolúveis será realizada por meio SDS-PAGE.

A proteína recombinante PNPase foi expressa na sua forma solúvel quando transformada em células de *E. coli* BL21pLys a 37º C durante 5h de crescimento com indução de 1mM de IPTG (Figura A3).

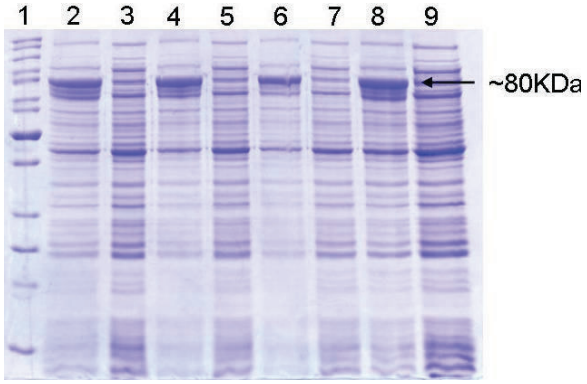

Figura A3: Análise por SDS-PAGE (12%) da expressão da fração solúvel da proteína PNPase. 1: Marcador Page Ruler; 2 e 3: 2 horas de crescimento PNPase e controle; 4 e 5: 3 horas de crescimento PNPase e controle; 6 e 7: 4 horas de crescimento PNPase e controle; 8 e 9: 5 horas de crescimento PNPase e controle; as amostras foram induzidas com 1mM de IPTG

Após obtenção da proteína na fração solúvel, as células foram cultivadas em maior escala através do método desenvolvido por Jones e colaboradores (2003). As células cultivadas foram ressuspendidas em tampão A (Tris-HCl 50mM pH 7.6), 10ml de tampão por grama de célula e rompidas através da ação de lisozima combinada com um detergente zwitterionico CHAPS. A fração solúvel foi tratada com DNase a fim de precipitar os ácidos nucléicos. Após o rompimento e o tratamento com DNase, a amostra foi centrifugada e dialisada contra o tampão A onde foi adicionado 10mM de fosfato de potássio, tanto dentro quanto fora da amostra dialisada. Essa diálise foi a 37ºC sob agitação, afim de que a enzima catalise a reação de fosforólise e libere os ácidos nucléicos que ainda estejam complexados na enzima PNPase. Após essa diálise, a amostra foi aplicada em uma coluna de troca iônica Q-Sepharose Fast flow de 70ml pré-equilibrada com o tampão A, onde um gradiente linear de 0 a

100% de tampão B (tampão A mais 400mM de NaCl) foi aplicado. A proteína eluída foi aplicada numa coluna de exclusão por tamanho Sephacryl S-300 pré-equilibrada com tampão A, e posteriormente numa coluna de troca iônica de alta resolução MonoQ 16/10, onde foi aplicado um gradiente de 0 a 100% de tampão B e obtivemos a proteína recombinante na forma homogênea.

A fim de determinar a concentração total de proteína foi utilizado método de Bradford (Bradford, 1976). A curva-padrão foi realizada utilizando albumina de soro bovino, onde todos os pontos da curva foram feitos em triplicata. A análise do método de Bradford mostrou que a partir de 5 gramas de células iniciais foram obtidos 10 miligramas de proteína após esse protocolo de 3 etapas cromatográficas.

REFERÊNCIAS BIBLIOGRÁFICAS

Bradford M M, A rapid and sensitive method for the quantitation of microgram quantities of protein utilizing the principle of protein-dye binding. ***Anal. Biochem.***, 1976; **72**;248-254

Bradley P, Jones G H, Overexpression of the polynucleotide phophorilase gene (pnp) of *Streptomyces antibioticus* affects mRNA stability and poly(A) tail length but not ppGpp levels. **Microbiology**. 2003; 149:2173-2182.

Clements M O, *et al.,* Polynucleotide phosphorilase is a global regulator of virulence and persistency in *Salmonella enterica*. **PNAS.** 2002; 99:8784-8789.

Coburn G A, Mackie G A, Degradation of mRNA in Escherichia coli: and old problem with some new twists. **Prog. Nucl. Acids. Res. Mol. Biol.** 1999; 62:55-105.

Godefroy-Colburn T, Grunberg-Manago M, Polynucleotide phosphrylase. **The Enzymes**. 1972; 7:533-574.

Grunberg-Manago M, Ochoa S, Enzymatic synthesis and breakdown of polynucleotides: polynucleotide phosphorylase. **J. Am. Chem. Soc**. 1955; 77:3165-3166.

Jones G H, Symmons M F, Hankins J S, Mackie G A, Overexpression and purification of untagged polynucleotide phosphorylases. **Protein Expr Purif.** 2003; 32:202-209.

Littauer U Z, Soreq H, Polynucleotide phosphorylase. **The Enzymes**. 1982; 15:517-553.

Littauer U Z, From polynucleotide phosphrylase to neurobiology. **J Biol Chem.** 2005; 280 (47):38889-38897.

Mitra S. et al., *In vitro* processing activity of *Bacillus subtillis* polynucleotide phosphorilase. **Mol Microbiol**. 1996; 19:329-342.

Mohanty B K, Kushner S R, Polynucleotide phosphorilase both as 3`-5` exonuclease and poly(A) polymerase in *Escherichia coli*. **PNAS**. 2000; 97:11966-11971.

Pasqualoto K F, Ferreira E I, An approach for the rational design of new antituberculose agents. **Curr Drug Targets**. 2001; 427-37.

Sulewski M, Marchese-Ragona S P, Johnson K A, Benkovic S J, Mechanism of PNPase. **Biochemistry (Moscow).** 1989: 28:5855-5864.

Zahrt T C, Molecular mechanisms regulating persistent *Mycobacterium tuberculosis* infection. **Microbes Infect.** 2003; 5: 159-167.